

**Integrated Deep Learning and Bayesian Classification for  
Prioritization of Functional Genes in Next-Generation  
Sequencing Data**

**Chan Khai Ern, Edwin**

A thesis submitted to the  
Department of Biochemistry  
National University of Singapore  
in partial fulfilment for the  
Degree of Bachelor of Science with  
Honours in Life Sciences

Life Sciences Honours Cohort  
AY2015/2016 S1



## **DECLARATION**

I hereby declare that this thesis is my original work and it has been written by me in its entirety. I have duly acknowledged all the sources of information which have been used in the thesis.

This thesis has also not been submitted for any degree in any university previously.

---

Chan Khai Ern Edwin

04 April 2017

## **Acknowledgements**

This thesis would not have been possible without the guidance and support of Dr Kenneth Ban. I have really enjoyed working on this project, and I am very grateful that he gave me the opportunity to try something even though I was not familiar with the field.

# Table of Contents

## Contents

<b>1</b>	<b>Introduction</b>	<b>2</b>
1.1	Next Generation Sequencing (NGS) for Clinical Genomics . . . . .	2
1.2	Variant Calling of NGS Data . . . . .	2
1.3	Ensemble Methods for Improving the Accuracy of Variant Calling . . . . .	4
1.4	Deep Learning for Improving the Accuracy of Variant Calling . . . . .	5
1.5	Prioritisation of Variants with Bayesian Networks . . . . .	7
1.6	Aims and Approach . . . . .	9
<b>2</b>	<b>Materials and Methods</b>	<b>10</b>
2.1	Overall Experimental Approach . . . . .	10
2.2	Implementation of Computational Pipelines . . . . .	11
2.2.1	Workflow Management of Pipelines . . . . .	11
2.2.2	Preprocessing and Analysis . . . . .	12
2.2.3	Implementation of Deep Learning Networks . . . . .	12
2.2.4	Bayesian Network Ranking of Mutations . . . . .	12
2.3	Synthetic Datasets . . . . .	13
2.4	Alignment and Variant Calling of Sequence Reads . . . . .	13
2.5	Feature Engineering . . . . .	13
2.6	Patient Derived Xenograft Mouse Model Development and Sequencing . . . . .	16
<b>3</b>	<b>Results</b>	<b>17</b>
3.1	Generation of Synthetic Datasets . . . . .	17
3.2	Feature Engineering . . . . .	18
3.3	Variant Calling and Concordance . . . . .	18
3.4	Network Architecture . . . . .	20
3.5	Network Tuning and Optimisation . . . . .	23
3.5.1	Number of Layers . . . . .	23
3.5.2	Optimiser and Learning Rates . . . . .	25
3.5.3	Sample Balancing . . . . .	27
3.6	Benchmarking of Optimised Network with the Synthetic Dataset . . . . .	28
3.7	Benchmarking of Optimised Network with NA12878 Reference Dataset . . . . .	30
3.8	Ranking of Functionally Important Mutations using a Bayesian Network . . . . .	32
3.9	Validation of Bayesian Network Ranking of Mutations in a Patient-Derived Xenograft Cancer Model . . . . .	33

<b>4 Discussion</b>	<b>38</b>
4.1 Adapting Deep Learning for Improving Variant Calling Accuracy . . . . .	38
4.2 Improving Performance of Deep Learning Approach . . . . .	39
4.3 Improvements to Bayesian Network . . . . .	40
4.4 Clinical Usage of Bayesian Networks in Gene Prioritisation . . . . .	41
4.5 Future Directions . . . . .	42
4.6 Conclusion . . . . .	42
<b>5 Appendixes</b>	<b>43</b>
5.1 Neural Network Learning . . . . .	43
5.1.1 Feedforward Phase . . . . .	43
5.1.2 Backpropagation Phase . . . . .	44
5.1.3 Cost Function in Gradient Descent . . . . .	45
5.2 Feature Engineering . . . . .	47
5.2.1 Base Information . . . . .	47
5.2.2 Sequencing Biases and Errors . . . . .	48
5.2.3 Calling and Mapping Qualities . . . . .	49
5.3 Mathematical and Statistical Tools . . . . .	51
5.3.1 Derivation of F1 Score . . . . .	51
5.3.2 Principal Components Analysis (PCA) . . . . .	52
5.3.3 Synthetic Minority Overrepresentation Technique (SMOTE) . . . . .	53
<b>6 Bibliography</b>	<b>54</b>
<b>7 Relevant Code</b>	<b>66</b>
7.1 generate_matrixes.py . . . . .	66
7.2 train_network.py . . . . .	75
7.3 compute_bayesian.py . . . . .	85

## Abstract

The advent of next-generation sequencing technology has enabled large-scale interrogation of the genome to identify variants in patient samples. The accurate identification of functional variants can provide critical insights into the disease process to guide diagnosis and treatment. However, the use of clinical genomics remains limited as (i) the accurate identification of variants remains suboptimal, and (ii) the large number of variants identified may be difficult to interpret without a systematic approach of ranking by functional importance.

Here, we describe the development of a deep learning neural network to improve the accuracy of variant-calling, and a Bayesian classification method for the probabilistic ranking of functionally relevant genes. We show that an optimised neural network can call variants more accurately than single variant callers or concordant callers, with F1 score improvements of 6 percent in synthetic datasets and 4.5 percent in real datasets over the best concordant methods. Following the identification of high confidence variants, we further demonstrate that a Bayesian classification system can rank functionally relevant genes in a Diffuse Large B-Cell Lymphoma (DLBCL) patient sample.

We propose that the combined use of deep learning and Bayesian network analysis could be extended to build an analytical pipeline for clinical use to augment diagnosis and treatment of diseases by identifying high-confidence variants and ranking them systematically.

# 1 Introduction

## 1.1 Next Generation Sequencing (NGS) for Clinical Genomics

There has been a growing interest in using a patient's genome to guide the diagnosis and treatment of diseases (Rehm, 2017; Angrist, 2016), based on the fundamental intuition that variants and mutations in the genome alter gene functions that drive the initiation and progression of the disease. In oncology, for example, identification of the key driver mutations has been shown to be useful in stratifying cancer subtypes (Stratton, Campbell & Futreal, 2009), and identifying mutations for targeted therapy (Janitz, 2011). Furthermore, the development of next generation sequencing (NGS) technologies has dramatically reduced sequencing costs (Metzker, 2010; Mardis, 2008), enabling the adoption of genomic sequencing in clinical labs.

Although clinical genomics holds great promise, there are still two critical issues that limit its use in a clinical setting. Firstly, it is often difficult to obtain high-confidence variant calls from sequencing data, and secondly, the large number of variant calls for patient samples makes interpretation difficult for clinical decision-making.

## 1.2 Variant Calling of NGS Data

In variant calling, genomic DNA is fragmented, and the short reads are sequenced in a massively parallel manner using next generation sequencing technologies such as sequencing by synthesis. These reads are aligned to a reference genome, and variations in the DNA sequence, such as single nucleotide variants (SNVs) and insertions/deletions (indels) are identified by comparing the different reads aligned to the reference genome (Figure 1).

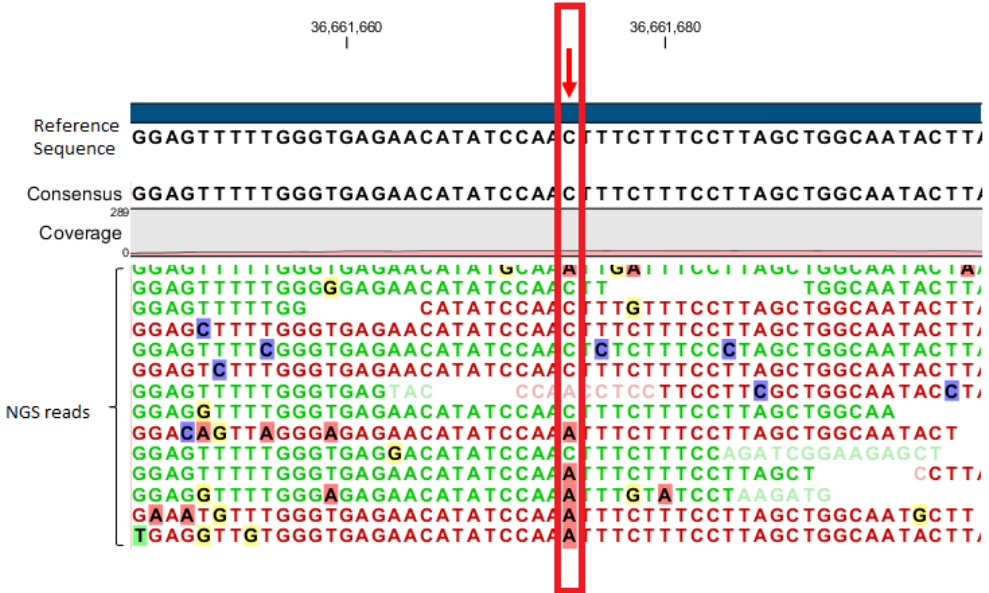


**Figure 1: Illustration of Variant Calling Pileup.** Due to noise and errors in sequencing and read mapping, it can be difficult to call variants accurately. At the position of interest, there seems to be a possible mutation from the original base of Cytosine to the base Adenine, but not all reads agree with this mutation call. Figure adapted from CLC Genomics Workbench 9.5, Figure 29.8.

Variant calling with NGS data primarily involves the use of various statistical and algorithmic methods to identify variants in the genome (Nielson et al., 2011). These variants represent the deviations and differences between the genome of interest and a reference human genome. This analysis is non-trivial as each variant call requires the integration of multiple sequence reads (e.g. millions of reads) that contain experimental noise and errors (Zook et al., 2014). The calling of variants can be further complicated by errors in mapping the reads to a reference genome.

To account for these errors, variant callers employ a variety of algorithms and statistical models to determine the existence and type of variation/mutation (Zook et al., 2014; Davey et al., 2011). Because of the differences in assumptions and models employed by different variant callers, certain calling algorithms are more sensitive and accurate in calling specific classes of variants but do not perform well in calling other variant types (O’Rawe et al., 2013). To address these problems, ongoing efforts have focused on improving current variant calling algorithms, including optimisation of variant calling for different classes of mutations, as well as the reduction in the number of false positive calls (Mohiyuddin et al., 2015; Gézsi et al., 2015).

Despite the variety of approaches used for identifying variants and mutations, the accuracy and

precision of single variant callers remain suboptimal (Cornish and Guda, 2015; O’Rawe et al., 2013). Each variant caller can differ greatly in accuracy depending on the type of sequencing methodology and the statistical algorithm used (Figure 2), making it difficult to identify true high-confidence variant calls.

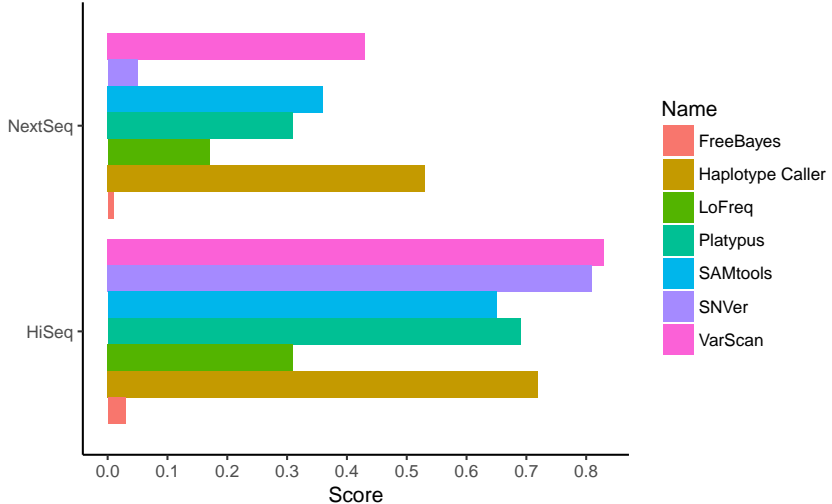


**Figure 2: Performance of Variant Calling Tools on Patient Data using the HiSeq and NextSeq Illumina Sequencing Platforms .** The F1 score indicates how well a caller can predict true positives (See Appendix 5.3 for more details). Notably, the F1 score for the same variant calling tool can differ greatly. Figure adapted from Sandmann et al. (2017)

### 1.3 Ensemble Methods for Improving the Accuracy of Variant Calling

While it is clear that single variant callers may not perform well across a variety of variant classes, the combination or ensemble of several callers can be used to augment the accuracy of variant callers beyond what can be achieved with a single caller. By aggregating the calls from each different variant caller, the relatively weak prediction calls from each caller can be combined to provide a better aggregate prediction for a variant call.

One simple approach to aggregating variant calls is by concordance, where the likelihood of an accurate call depends on multiple variant callers identifying the same variant or mutation (Lam et al., 2012; Wei et al., 2011). While straightforward and intuitive, the recall rates of such a tool is poor with a high number of false negative calls. This is because a high concordance of variant calls will reciprocally decrease the number of true variants calls that are identified by specific variant callers (O’Rawe et al., 2013).

Beyond concordance, supervised machine learning approaches have been used to combine the calls from different variant callers to improve calling accuracy. In these methods, machine learning algorithms have been used to predict the accuracy of a variant call by integrating different features of each variant call (e.g. variant frequencies, mapping quality). For example, the support vector machine (SVM) algorithm was used successfully to improve the accuracy of variant calls (Gézsi et al., 2015) over concordance-based methods.

Recent advances in machine learning, in particular, deep learning neural networks, have increased the accuracy of predictions from complex multi-modal data (Schmidhuber, 2015) beyond traditional algorithms such as SVM and Random Forests. The ability of deep learning networks to learn from complex high-dimensional data suggests that they may be useful in improving the accuracy of high-confidence variant calls derived from the complex features from each variant caller.

#### 1.4 Deep Learning for Improving the Accuracy of Variant Calling

Deep learning is a machine learning approach based on artificial neural networks (LeCun et al., 2015) that are built on artificial neurons. Each artificial neuron is analogous to a biological neuron where weighted input signals are integrated to produce an output once the signals cross a threshold for activation (Figure 3).

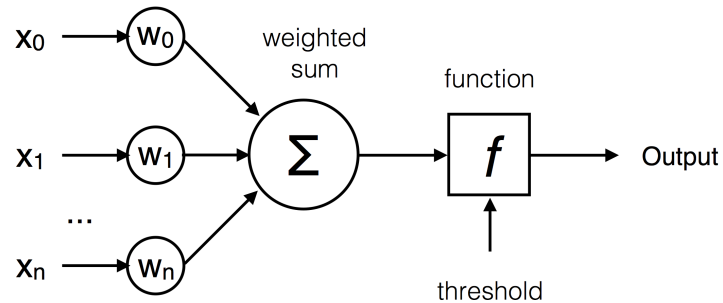
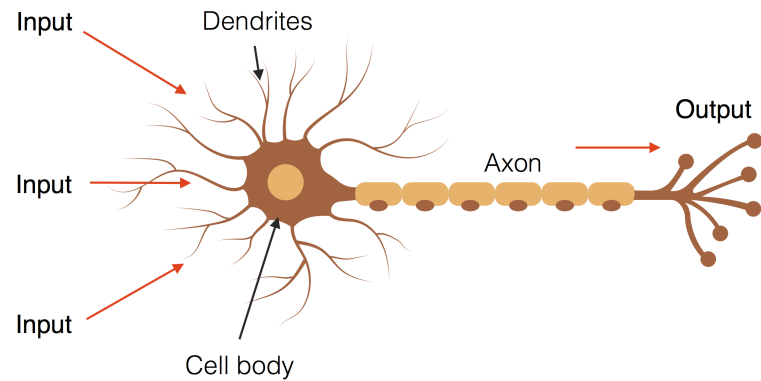
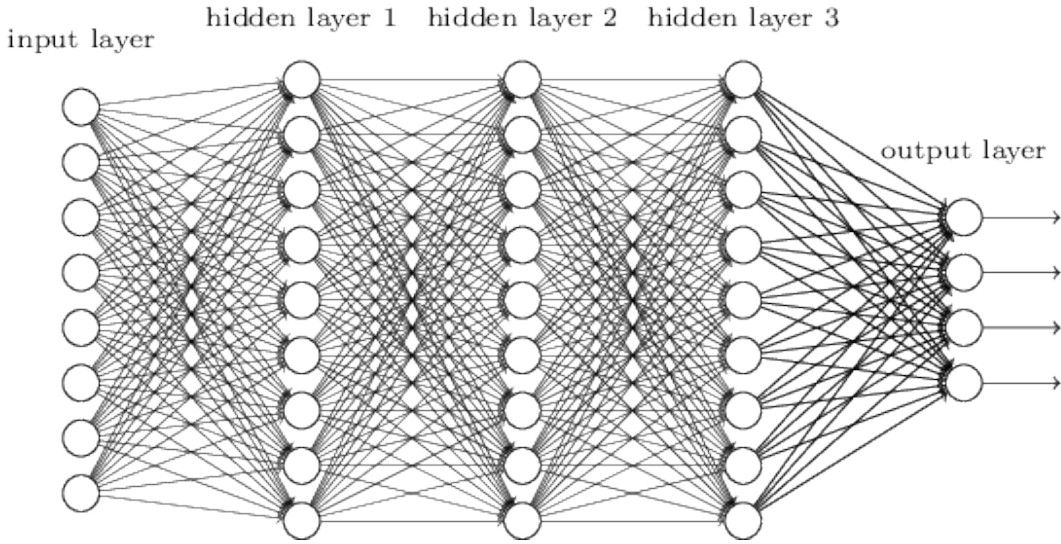


Figure 3: **Artificial Neurons as Building Blocks of Neural Networks**

In a deep learning network, the artificial neurons are connected in layers, comprising an input layer, an output layer, and a variable number of intermediate hidden layers (Figure 4). Here, the outputs of the neurons in one layer are connected to the inputs of next layer of neurons, with the weights of the connections determining the strength of signal propagation from one neuron to another.



**Figure 4: Sample Neural Network with Five Layers, Including Three Hidden Layers.** This diagram represents a densely connected neural network, where each node is connected to every node of the preceding and subsequent layers.

Deep learning networks can be trained by providing labelled data, where features of the dataset are fed into the input layer to produce the output prediction. By comparing the output to the actual labels, the network can be trained by adjusting the weights that determine the propagation of a signal from one neuron to the next. In this way, a trained neural network can predict the output when given new data (for a more detailed explanation, see Appendix 5.1).

Because deep learning networks contain multiple layers, they can learn different features in a hierarchical manner. This allows the network to solve complex non-linear decision boundary problems, including drug molecule solubility (Lusci et al., 2013), facial recognition (Sun et al., 2014) and even predicting the best move in the Japanese board game, Go (Silver et al., 2016). Given this ability to learn from complex features, deep learning networks provide a possible approach to improve the prediction high-confidence variant calls from an ensemble of different variant calling algorithms.

## 1.5 Prioritisation of Variants with Bayesian Networks

Once high-confidence variant calls can be established, there remains the second problem of identifying the functional importance of each variant/mutation, given that there are multiple variants in a typical genome (Shen et al., 2013). The ability to systematically prioritise and rank clinically significant variants would allow clinicians to focus their attention on relevant candidate mutations that can guide decision-making on diagnosis and treatment.

The problem of prioritisation of genetic variants and mutations arises from the multiplicity and complexity of data sources that can be utilised to determine the clinical and functional relevance of a variant or mutation in a gene (Moreau & Tranchevent, 2012). Several approaches have been used, including characterising variants and their phenotypes in clinical cases, and determining if a variant/mutation will alter protein function based on amino acid changes in conserved regions. Although these functional annotations of variants and mutations can be performed with tools such as ANNOVAR (Wang, Li, & Hakonarson, 2010), the fundamental problem of integrating the information in a systematic manner remains.

One possible approach to addressing this problem is by using Bayesian networks to probabilistically integrate diverse information sources to predict the likelihood of an outcome. This approach has been successfully used in solving a variety of decision making problems (Pourret et al., 2008; Jensen et al., 1996), including medical treatment decision making (Windecker et al., 2014), ecological studies (Johnson et al., 2014) and predictive epidemiology (Su et al., 2014).

In a Bayesian network, the probabilities of different events can be linked so that the final likelihood of an outcome can be evaluated. An example of a simple Bayesian network is shown in Figure 5. Here, the likelihood of the outcome, which is rain, is dependent on the probabilities of thunder, cloudy day and the weather forecast. The probabilities of the variables can be used to update the final likelihood of the outcome, based on the conditional probabilities of thunder, cloudy day, and weather forecast. In a similar way, the probability of a functionally important variant/mutation can be evaluated based on the conditional probabilities of the functional annotation and confidence of a true variant call.

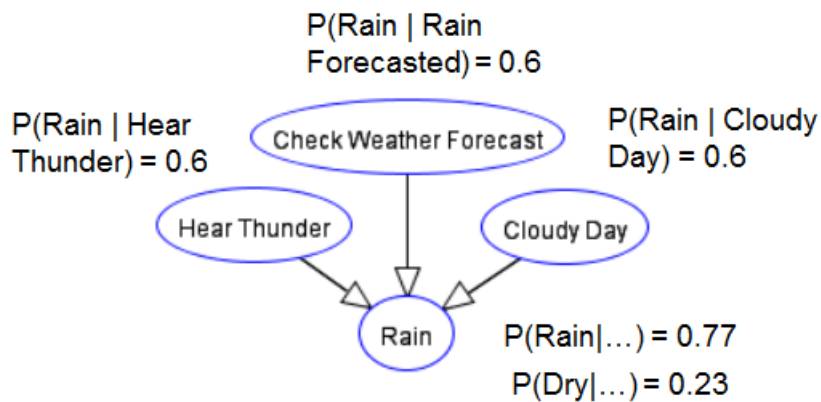


Figure 5: Sample Bayesian Network for Rain Prediction.

One advantage of Bayesian network analysis is that it approximates how humans reason about relationships between events and outcomes - we observe events and update our probabilistic estimates of the likelihood of an outcome. Additionally, because Bayesian networks require the explicit specification of relationships between the events and the outcome, the model is transparent and can be built based on known relationships between events, based on existing knowledge.

Bayesian networks are well suited to ranking the importance of functionally important variants/mutations because the model can be built using the explicit specification of the probabilities accounting for the high confidence calls and the predicted functional effects of the variants/mutations. This explicit specification permits a better understanding of the ranking process, which is important for clinical decision-making.

## 1.6 Aims and Approach

The overall goal of this project is to address the two major issues limiting the utility of clinical genomics through the following aims:

1. To develop and validate a deep learning network model for improving the accuracy of variant calling.
2. To develop a Bayesian network model for ranking functionally important variants/mutations from high confidence calls identified by the deep learning network.

We describe the development of (i) a deep learning network to identify high-confidence variant calls (focusing on SNVs and short indels) and (ii) a Bayesian network to probabilistically prioritise their functional importance. As a first step, we developed and optimised a deep learning network to identify true variants in both synthetic and real-world datasets. Following the identification of high-confidence variant calls, we built a Bayesian network ranking system based on functional annotations to prioritise mutations and used it to identify functionally important mutations in a cancer sample.

## 2 Materials and Methods

### 2.1 Overall Experimental Approach

As a first step in the development of deep learning networks for variant calling, we built two main computational pipelines : (i) a training pipeline for training and the optimisation of the neural network, and (ii) an analysis pipeline that uses a trained neural network to perform variant prediction and validation (Figure 6).

In the training pipeline, training datasets from synthetic and real sequencing data were used for performing the processing steps of alignment, variant calling and training of the deep learning network. Briefly, FASTQ sequence reads were first mapped to the reference genome before variant calling was performed using an ensemble of callers. The different variant callers were used to generate the feature vectors that served as the input for the deep learning network. The predictions by the neural network were compared to the ground truth variant calls to train the network to predict high confidence variants.

In the analysis pipeline, the trained and optimised network from the training pipeline is then used to predict high-confidence variant calls in naive samples without ground truth variant calls. In brief, the FASTQ sequence reads are aligned and variant calling performed in a similar fashion as in the training pipeline. The feature vectors from the ensemble of callers is used to predict high confidence calls using the trained and optimised deep learning network.

Finally, we applied the Bayesian network analysis to rank the functionally important variants/mutations from the high confidence calls identified from naive samples in the analysis pipeline.

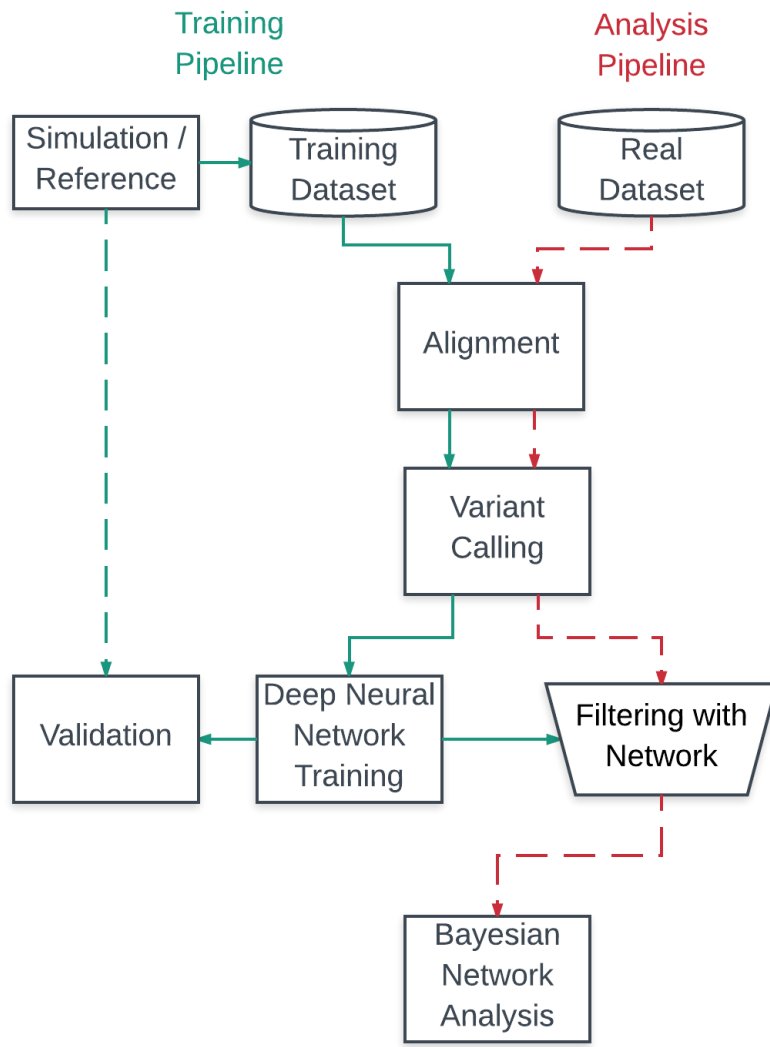


Figure 6: **Overall Structure of Computational Pipelines.** The pipelines were implemented using NextFlow, a domain-specific language for workflows

## 2.2 Implementation of Computational Pipelines

### 2.2.1 Workflow Management of Pipelines

The workflows in the training and analysis pipelines were managed using NextFlow (v0.21.3.3990), a Groovy based Domain Specific Language (DSL) that provides easy management of parallel pipelines consisting of dependent tasks organised as a directed acyclic graph (Tommaso et al., 2014). Nextflow was used to manage and coordinate the different steps in the pipelines to ensure reproducibility and scalability.

### **2.2.2 Preprocessing and Analysis**

The preprocessing and analytical components were implemented using Python (v2.7) (Van Rossum, 2007) and the following Python libraries: NumPy, scikit-Learn, Pomegranate and PyVCF. Briefly, NumPy (v1.11.3) was used to prepare feature vectors for deep learning training, scikit-learn (v0.18.1) was used to perform Principal Component Analysis (PCA) and Synthetic Minority Oversampling Technique (SMOTE) methods (See Appendix 5.3 for details). PyVCF (v0.6.8) was used to parse the VCF files to facilitate the comparison of variants efficiently in  $O(1)$  time using hash-based dictionary lookups.

### **2.2.3 Implementation of Deep Learning Networks**

Deep learning networks were implemented using the Keras library (v1.1.1) with a TensorFlow backend (v0.11.0). TensorFlow, from Google (Abadi et al., 2015), was used for better network training performance due to its distributed computation and queue management system. For each of the network architectures, we used the LeakyReLU activation function. The LeakyReLU is a refinement of the ReLU activation function which minimises the "dying ReLU" problem, and both are well-documented activation functions that have been shown to work well in deep neural networks (Anthimopoulos et al., 2016; LeCun, Bengio & Hinton, 2015; Maas, Hannun & Ng, 2013). Additionally, dropout filters were used to prevent overfitting of data (Srivastava et al., 2014).

The code used to generate the feature vectors and train the neural network can be found in Relevant Code – Section 7.1 and 7.2 respectively. Details on the algorithms used in deep learning can be found in Appendix 5.1.

### **2.2.4 Bayesian Network Ranking of Mutations**

For the Bayesian ranking of mutations, the high confidence calls from the deep learning network were annotated using ANNOVAR (v2015Jun17) (Wang, Li, & Hakonarson, 2010). The annotated features for each variant were used as inputs to the Bayesian network, which was implemented using Pomegranate (v0.6.1), a Python library for Bayesian analysis. The implementation code for the Bayesian network can be found in Relevant Code – Section 7.3.

## 2.3 Synthetic Datasets

Synthetic genomes enable the simulation of NGS data with ground truths to test and validate a neural network. For our simulator, we used Mason, a genome mutation software written in C++ (v2.3.1) to mutate the hg19 reference genome from UCSC (Karolchik et al., 2014). We used indel rates of 0.00002 and SNP rates of 0.00008 to generate sufficient truth variants for analysis, which comprise 229253 SNPs and 57257 indels.

After generating a ground truth model, we simulated sequence reads with error rates and ground truth variants (Figure 7). For error rates, we used published data from Schirmer et al. (2016) as the input to Mason – the general substitution error rate was 0.0004 per base in the genome, and the insertion and deletion error rate per base were  $5 * 10^{-6}$ .

## 2.4 Alignment and Variant Calling of Sequence Reads

The sequence reads (FASTQ) from synthetic or real datasets were first aligned to the hg19 human reference genome using BWA (0.7.13) (Li, 2013) using the default settings. Following alignment, the alignment files (BAM) were used for variant calling with the following callers with their default settings: FreeBayes (v1.0.2-16); GATK Haplotype Caller (v3.7-0) and Unified Genotyper (v3.7-0); Samtools (v1.3.1); Pindel (v2.3.0) (Garrison & Marth, 2012; McKenna et al. 2010, DePristo et al. 2011; Li H, et al., 2009; Ye et al., 2009). The overall process is shown in Figure 7.

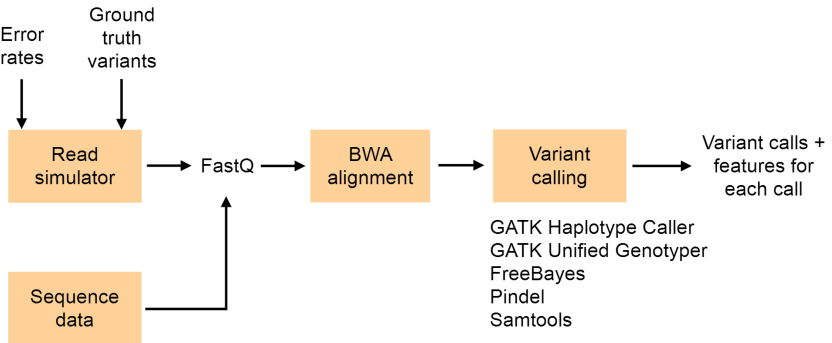


Figure 7: Overall Workflow of Generation of Synthetic Dataset, Alignment and Variant Calling

## 2.5 Feature Engineering

In order to train a neural network, features in the form of numerical vectors must be used as an input. We subset our features into three broad sets, which are base-specific information,

sequencing error and bias information features, and calling and mapping quality. The computation of the features was performed as described below. For an in-depth explanation of their usage and interpretation, see Appendix 5.2.

## Base Information

### Shannon Entropy

Shannon Entropy captures the amount of information contained in the allele sequences. It is calculated using the equation:

$$H(X) = - \sum_{i=1}^n P(x_i) \log_2 P(x_i) \quad (1)$$

where  $P(x_i)$  is the prior probability of finding each base at each position. This prior probability is calculated in two ways – over the entire genome and over a region of space around the allele (10 bases plus the length of the allele in our calculations).

### Kullback Leibler Divergence

The Kullback-Leibler Divergence feature is similar to Shannon entropy, but instead, we use this to measure the informational gain from the reference to the allele sequence. The Kullback-Leibler Divergence is calculated as follows:

$$D_{KL}(P||Q) = - \sum_{i=1}^n P(x_i) \log_2 \frac{P(x_i)}{Q(x_i)} \quad (2)$$

where  $Q(x_i)$  is the prior probability of finding each base at each position based on the genomic region around the allele, while  $P(x_i)$  is the posterior probability of finding a specific base inside the allelic sequence.

### Base Quality

Base quality refers to the Phred score probability that the called allele is wrong. It is given by the equation:

$$P = 10^{-\frac{Q}{10}}$$

Where P is the Base Quality, and Q is the probability that the allele called is wrong. This is a number computed by the sequencing machine based on the quality of the base samples provided.

## **Sequencing Biases and Errors**

### GC content

This feature comprises the GC content of the reference genome for at least ten bases around the mutation site.

### Longest homozygous run

This feature comprises the longest similar string of bases in the reference genome, for at least ten bases around the mutation site.

### Allele Count and Allele Balance

This feature is an output from Haplotype Caller and Unified Genotyper, and describes the total number of alleles contributing to a call and the balance between reference and alternate alleles reads.

## **Calling and Mapping Qualities**

### Genotype Likelihood

The genotype likelihood score provides the Phred-scaled likelihood scores of how confident the caller is in determining that it is a homozygous or heterozygous call, and is provided by all variant callers.

### Read Depth

Mapped read depth refers to the total number of bases sequenced and aligned at a given reference base position. It is provided by all variant callers.

### Quality by Depth

Quality by depth is computed by dividing the quality score against allele depth, to obtain an average score of allele quality. This is provided by Haplotype Caller and Unified Genotyper.

### Mapping Quality

Mapping quality is a score provided by the alignment method and gives the probability that a read is placed accurately. It is provided by all variant callers except Pindel.

## **2.6 Patient Derived Xenograft Mouse Model Development and Sequencing**

A patient-derived xenograft model of diffuse large B-Cell lymphoma (DLBCL) was performed by the Mouse Models of Human Cancer Unit (MMHCU) at the Institute of Molecular and Cell Biology (IMCB), in accordance with the approved protocols by the Institutional Review Board (IRB). In brief, a sample of the DLBCL tumour was implanted into NOD-SCID-gamma mice and serially propagated as a xenograft. The DNA from the xenograft was extracted for high-throughput sequencing using the Illumina HiSeq platform (Genotypic Technology, India). The sequence reads from the xenograft were used to validate the Bayesian network ranking of functionally important mutations.

### 3 Results

#### 3.1 Generation of Synthetic Datasets

As a first step towards developing a deep learning network, we generated a synthetic dataset containing known truth variants as labels for supervised learning (Escalona, Rocha & Posada, 2016). To do this, we generated a synthetic genome with mutations using the hg19 genome from UCSC (Karolchik et al., 2014) as a reference. The synthetic genome contains over 300,000 random mutations spread over the chromosomes (Figures 8 and 9). This genome was used to generate NGS sequence reads incorporating error profiles from the Illumina platform.

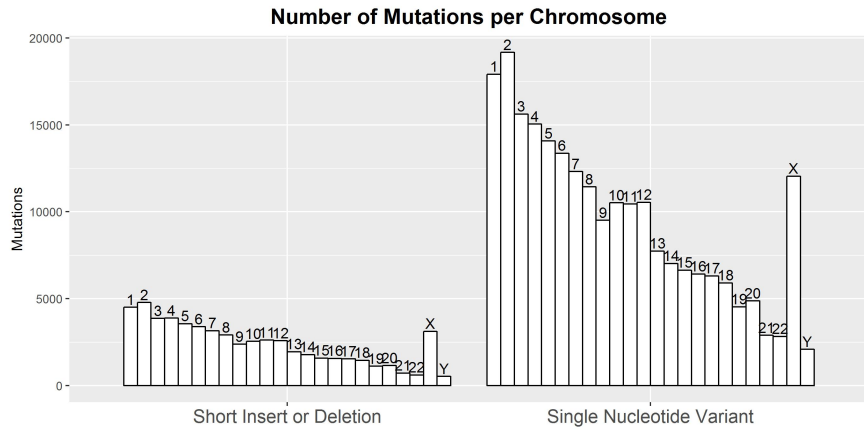


Figure 8: Number of Ground Truth Mutations (Variants) Created in Each Chromosome

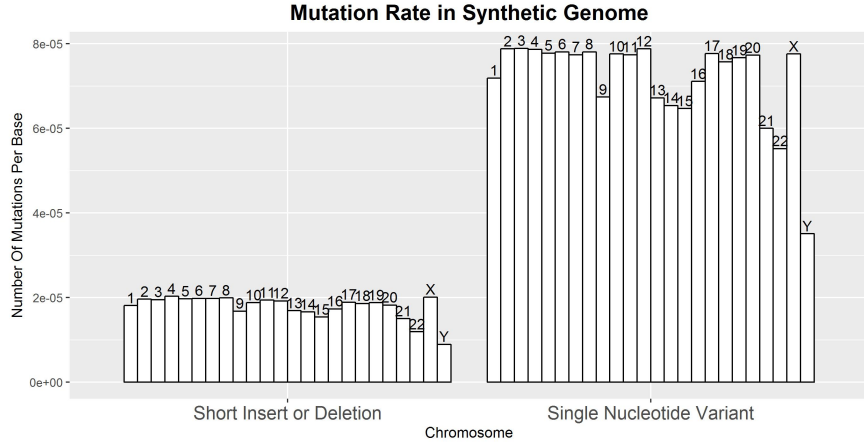


Figure 9: Mutation Rate per Base in Each Chromosome

## 3.2 Feature Engineering

Deep learning requires features to be vectorised and normalised to be used as input data. We assembled a set of 20 features, using data obtained from the variant callers themselves as well as engineering other features from the dataset. A summary of the features used in training can be found in Table 1, and a description of the full list of features can be found in Appendix 5.2.

Features were engineered based on obtaining information on the main aspects of variant calling, which includes the information contained in the sample bases (Base Quality, Entropy, Kullback–Leibler divergence, etc.), the confidence we have in the calling and alignment (Read Depth, Mapping Quality etc) and finally possible biases in the sequencing machine (Allele Balance, Allele Count, GC content).

Table 1: **Key Features Engineered from each Caller**

Features	Shannon Entropy (Reference, Alternate and KL- Divergence)	Base Composition (Homopolymer Run, GC content)	Read Depth	Mapping Quality	Base Quality	Allele Balance	Quality by Depth	Allele Count	Genotype Likelihoods
Free Bayes	+	+	+	+	+	+	+		+
Haplotype Caller	+	+	+	+	+		+	+	+
Unified Genotyper	+	+	+	+	+	+	+	+	+
Pindel	+	+	+						+
Samtools	+	+	+	+	+	+			+

## 3.3 Variant Calling and Concordance

For the training of the deep learning network, we used a mix of variant callers that use orthogonal calling and reference methodologies in order to maximise the information that the neural network can use for prediction (See Table 2).

We used two haplotype-based callers, FreeBayes (Garrison & Marth, 2012) and GATK Haplotype Caller (McKenna et al. 2010, DePristo et al. 2011), two position based callers GATK Unified Genotyper and Samtools (Li H, et al., 2009) and finally Pindel, a pattern growth based caller (Ye et al., 2009). When we analysed the concordance rates of the callers on the synthetic dataset, we found a high number of calls were not concordant, with many calls only identified by a minority of variant callers (Figure 10).

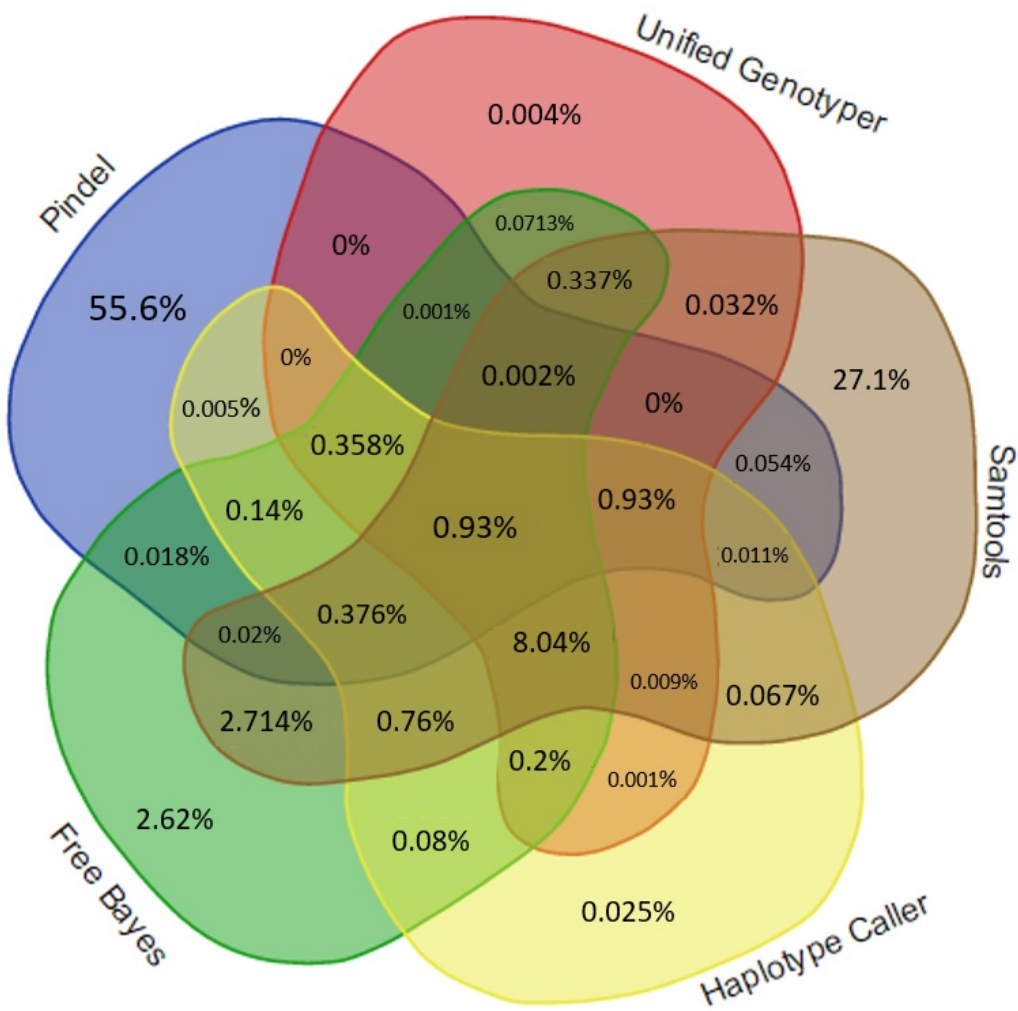


Figure 10: **Concordance of Callers on Synthetic Dataset**

We found that Pindel was the most discordant caller, with over 1.6 million (55.6%) unique calls that are different from other calls. Samtools was also discordant, with over 800 thousand unique calls (27.1%) that were unique from the other callers, followed by FreeBayes at 80,000 calls. These discordant calls are consistent with the different methodologies used by each variant (Table 2), leading to different calling profiles. Because of the high discordance of variant calls, identifying high-confidence calls by simple concordance is not likely to be optimal, but may be better handled by machine learning algorithms such as deep learning that can account for complex interrelationships.

Table 2: Comparison of Different Methods and Features of Variant Callers.

	GATK Unified Genotyper	Samtools	GATK Haplotype Caller	Free Bayes	Pindel
Calling Method	Uses a list of mapped reads, calling model is probabilistic with increased priors at regions with known SNPs	Uses a list of mapped reads, calling model is probabilistic. Does not assume sequencing errors are independent and has less hard filters compared to Unified Genotyper	Uses Hidden Markov Models to build a likelihood of haplotypes which are then used to call variants	Uses a posteriori probability model to build a set of haplotypes to represent mutations, calling model is probabilistic with population based priors	Locates regions which were mapped with indels or only one end was mapped, and then performs a pattern growth to find inserts and deletions. Shown to be able to identify medium length indels missed by other callers in real samples (Spencer et al., 2013)
Reference and Mapping Method	Position based caller that realigns fragments and analyses each position to call SNPs and indels	Position based caller that uses mapped sequences to call SNPs and indels.	Analyses regions where there is high likelihood of mutation based on activity score, and builds a De Bruijn-like graph that reassembles reads (Haplotypes) in that region	Dynamic sliding window based reference frame, using algorithms to determine window size for analysis. Does not require precise alignment, unlike other callers	Focuses on Unmapped regions, regions known to have insert and deletions or regions with only one end mapped.

### 3.4 Network Architecture

The deep learning network can be designed using different structures that may differ in performance depending on the characteristics of the input data. We tested out various neural network architectures to see which architecture would perform the best for our set of input features (Figure 11). In order to compare the performance of the different network architectures, we calculated the precision, recall and F1 score from the predicted variant calls in each network: (i) the precision score is defined as ratio of true positives over false positives and true positives; (ii) the recall score is the ratio of true positives over true positives and false negatives; and (iii) the F1 score is the harmonic mean of precision and recall. The derivations of these metrics can be found in Appendix 5.3.1.

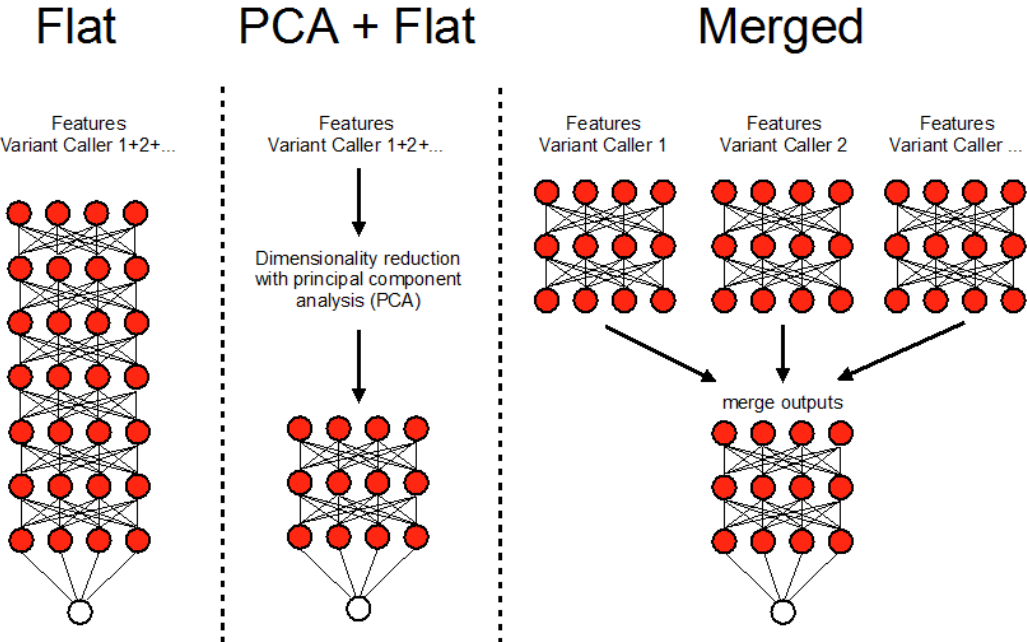


Figure 11: **Different Designs for Neural Network Architecture**

We first tested the commonly used flat architecture (Figure 11), which contains stacks of fully connected layers with multiple nodes, initially consisting of seven layers with 80 nodes per layer. In this architecture, all the features from the different variant caller were concatenated into a single vector and used as an input to train the neural network. We found that this architecture was not able to learn from the features, resulting in poor precision (0.0592) and F1 scores (0.111) (Figure 12), suggesting that the number of features might be too high for the flat architecture.

To address this, we explored the use of principal components analysis as pre-processing step to reduce the number of dimensions prior to the input layer of the flat neural network architecture. Principal components analysis (PCA) is a dimensionality reduction technique that enables a compressed representation of data (Chen et al., 2014; Van Der Maaten, Postma & Van den Herik, 2009). Each principal component is a linear summation of the original features

( $X$ ) in the form

$$PC_1 = \beta_{1,1} * X_1 + \beta_{2,1}X_2 + \dots + \beta_{n,1}X_n$$

...

...

$$PC_i = \beta_{1,i} * X_1 + \beta_{2,i}X_2 + \dots + \beta_{n,i}X_n$$

which enables a few principal components to capture a high amount of variance in the dataset.

By performing this procedure, we reduced the features to 8 principal components that we used for the inputs to the neural network. However, this reduction in features did not result in appreciable learning in the network, as evidenced by the poor precision (0.0734) and F1 scores (0.136) (Figure 12).

We reasoned that the architecture was not able to learn because of the multimodal nature of the features from each variant caller. To accommodate the multimodal data, we used a merged network architecture consisting of smaller subnets (five layers, 24 nodes per layer) for each variant caller, before merging the outputs in a common network produces the final prediction of a high-confidence variant call (Figure 11). Merged networks have previously been shown to be able to successfully integrate information from multi-modal datasets (Eitel, 2015; Suk, Lee & Shen, 2014). This architecture proved to be capable of integrating the various complex features, resulting in significantly higher precision (0.877) and F1 scores (0.929).

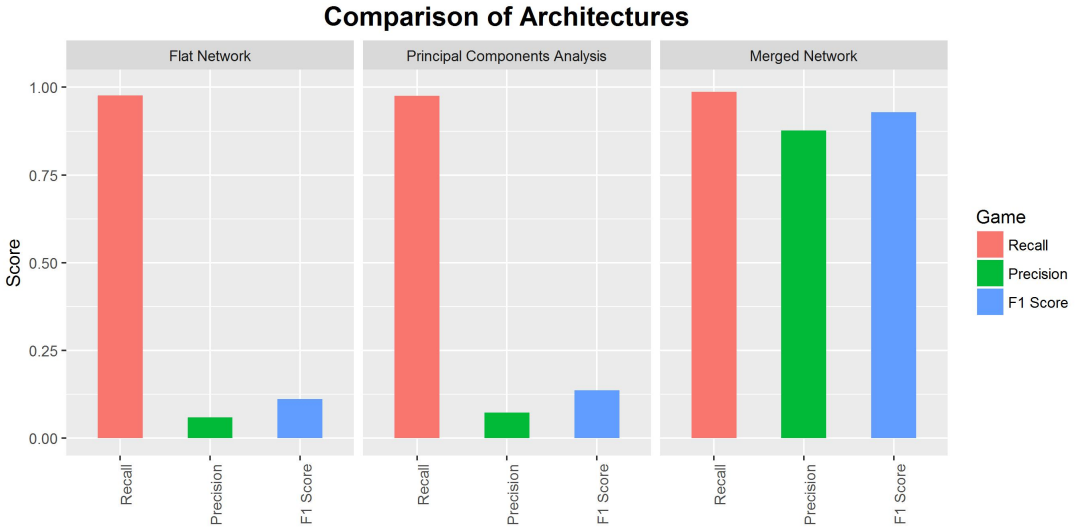


Figure 12: **Analysis of Different Neural Network Architecture**

In summary, we were able to identify a network architecture that could predict high-confidence variant calls from a synthetic dataset by addressing the multimodal nature of the data. The two other networks were not able to learn, resulting in poor precision and F1 scores. Interestingly, the recall scores for all three architectures were around the same ( $\pm 0.01$ ), indicating the main difference for the merged network architecture was in its ability to remove false positive calls.

### 3.5 Network Tuning and Optimisation

Next, we systematically optimised and tuned the deep learning neural network to maximise its predictive ability. To do this we focused on 4 parameters that are known to be critical in deep learning networks (Ruder et al., 2016; LeCun, Bengio & Hinton, 2015; Yan et al., 2015; Sutskever et al., 2013), specifically the (i) number of layers; (ii) optimiser choice, (iii) learning rate and (iv) balancing of positive and negative training samples.

#### 3.5.1 Number of Layers

Firstly, we evaluated how the number of layers affects the performance of the neural network, as the number of layers determines the representation of data that can be captured by the neural network. The number of layers can affect the network in two ways – increasing the number of layers can enable complex data representation needed for learning, but excessive layers might result in the vanishing gradient problem (Sutskever et al., 2013; Bengio et al.,

1994), where the signals are unable to propagate across too many layers.

Using our merged network architecture as a foundation (Figure 13), we varied the number of layers in the pre-merge networks that were specific for each caller and the common network after the merge layer.

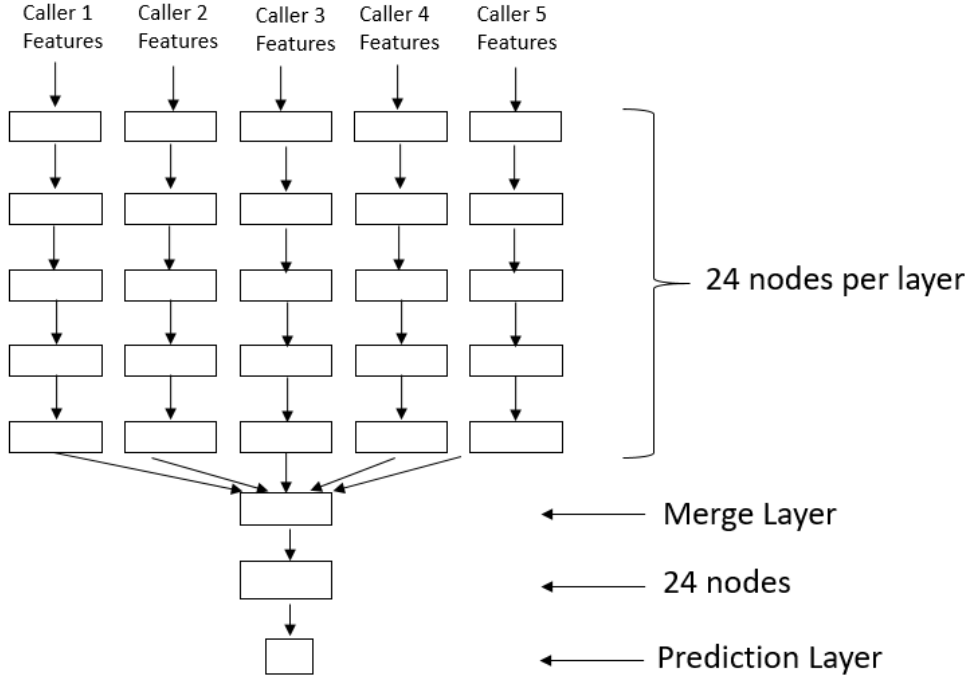


Figure 13: **Basic Merge Network Structure.** Each individual pre-merge layer takes in an input feature vector from a single caller. The information is then integrated in a set of merge layers to give a prediction.

We observed that changing the number of layers after the merge layer did not significantly vary the performance. Thus we focused on changing the number of layers before the merge layer. We compared six different neural network structures (four layers to nine layers) using accuracy as the main metric, which is defined as the fraction of all samples that the neural network can correctly predict.

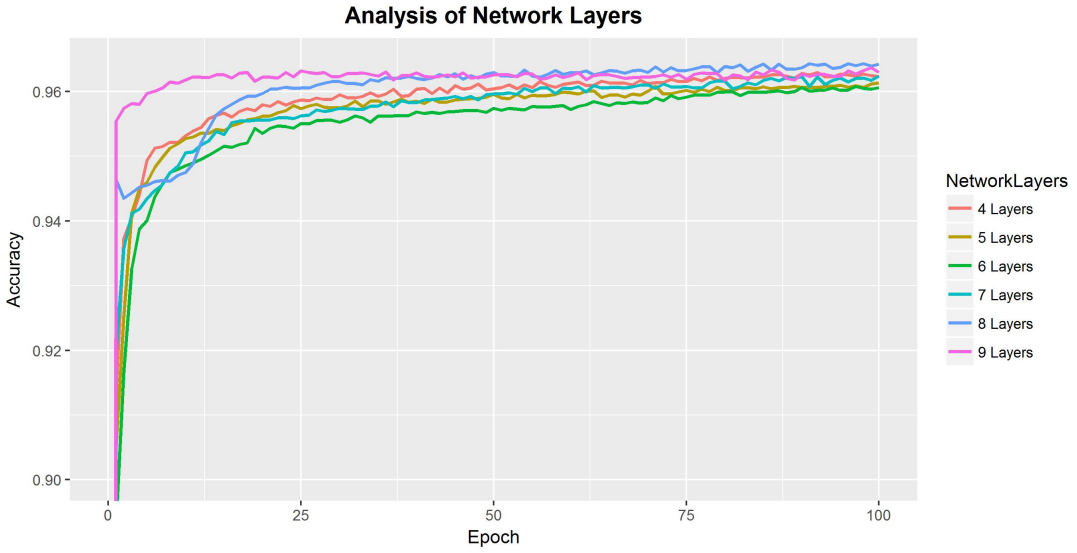


Figure 14: **Analysis of Different Number of Layers On Training Accuracy**

We found that all the different layered network were able to learn, but the eight layer neural network performed the best at learning from the input data, with a final accuracy of 0.964 that was approximately 0.001 higher than other layers.

### 3.5.2 Optimiser and Learning Rates

Next, we sought to choose the best optimiser and learning rate for our eight-layer network. Both optimisers and learning rates have been shown to be important in neural network training (Ruder et al., 2016; Sutskever et al., 2013).

Optimiser choice is critical as the optimisers determine how the weights and gradients are updated in the network, thus playing an integral part in learning. We evaluated three standard optimisers for use in our network, ADAM, RMSprop and Stochastic Gradient Descent (SGD). ADAM is an adaptive learning rate optimiser that is known to be well suited in large dataset and parameter problems (Kingma & Ba, 2014). RMSprop is another adaptive learning rate optimiser that has been shown to work well for real experimental datasets (Tieleman & Hinton, 2012). SGD is the simplest learning model with no adaptive learning rate but is a useful model because it is the easiest to understand mathematically and has also been shown to solve deep learning problems (Kingma & Ba, 2014). Further information on the mathematical foundations of optimisation and backpropagation, can be found in Appendix 5.1.

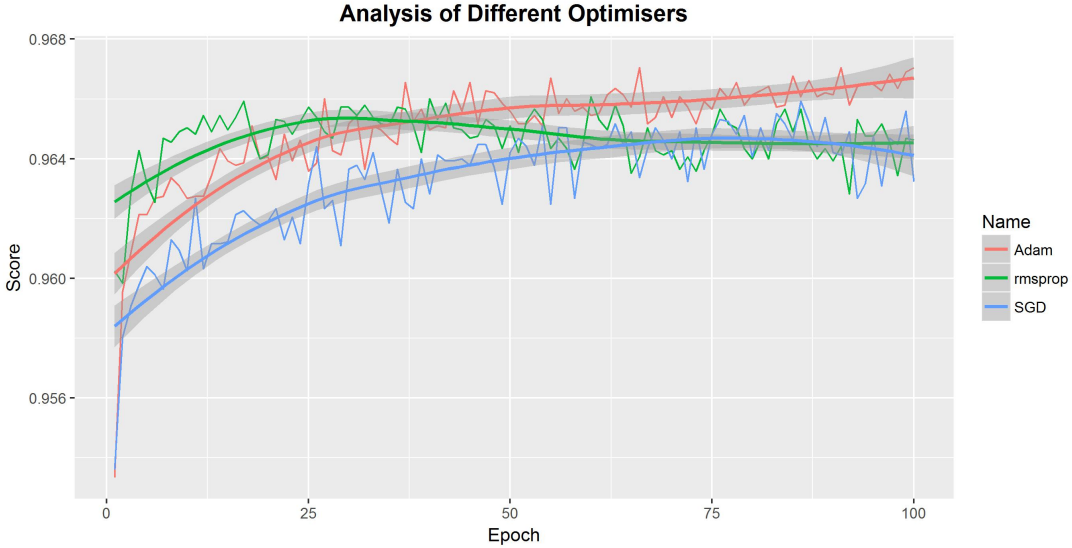


Figure 15: **Optimiser Accuracies for Training at each Epoch.** Due to the accuracy noise, the overall momentum of the dataset, calculated as a sliding window average is shown. The 95% confidence interval is also shown.

We evaluated the accuracy of the neural network running on each of the three optimisers (Figure 15). We found that Adam obtained the highest accuracy of 0.9670, while RMSprop and SGD reached maximum accuracies of 0.9660 and 0.9569 respectively. Interestingly, the adaptive rate optimisers seemed to have complex learning trajectories, while SGD has a very stable learning rate. This is consistent with that fact that adaptive learning rates allow greater gradient descents when the error is high while decreasing the learning rate when the error is low (Kingma and Ba, 2014; Zeiler, 2012). This adaptive capacity enables Adam and RMSprop to learn at variable rates based on the current gradients. In contrast, SGD requires more time to learn the true minima, but eventually still reaches about the same minima as RMSprop.

We chose Adam as our optimiser as (i) the final accuracy discovered by Adam was noted to be higher than RMSprop and SGD, and (ii) the learning curve for Adam was stable, indicating it is able to learn and update the gradients in the neural network to learn from input data at all epochs.

Finally, we evaluated initial learning rates for the Adam optimizer (Figure 16). We found that the most stable learning trajectory was observed at a learning rate of  $10^{-5}$ . This initial learning rate is critical as it determines the first few gradient descents which enable stable adaptive learning throughout the epochs (Sutskever et al., 2013). At higher learning rates ( $10^{-4}$  and below), a very high amount of noise was observed, indicating that the learning rate

was too high resulting in a difficulty in finding the minima. At lower learning rates ( $10^{-6}$  and above), the final accuracy after 100 epochs (0.9639 for  $10^{-6}$ ) was lower than the learning rate at  $10^{-5}$  (0.9672). Thus, we concluded that  $10^{-5}$  was the optimal learning rate for our network.

**Analysis of Different Learning Rates**

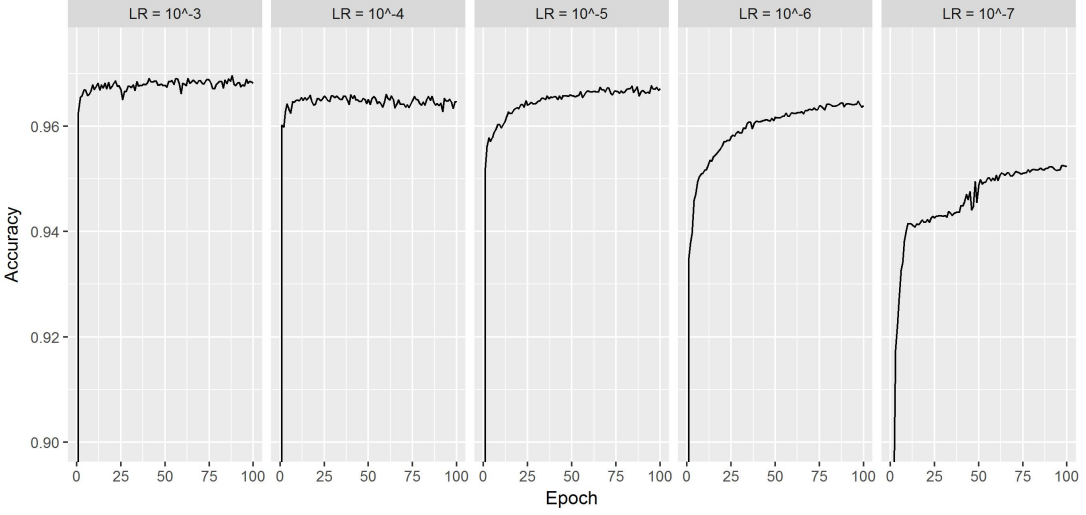


**Figure 16: Training Accuracies over Each Epoch for Different Learning Rates**

### 3.5.3 Sample Balancing

We then considered whether the imbalance in samples would affect the performance of the network, given the synthetic dataset contained an abundance of negative training examples compared to positive training examples. In total, there were 286,510 positive training examples and 4,547,919 negative training examples (about a 15-fold difference). Sample imbalances in the training data have been known to affect learning adversely, particularly if the minority class is the class we are interested in predicting accurately (Yan et al., 2015; López et al., 2012). Thus, we wanted to determine if correction of imbalances would improve network performance by using two different methods of sample balancing: undersampling and oversampling. In the undersampling approach, negative training examples were removed until the number of negative training examples was equal to the number of positive training examples. In oversampling approach, we used that Synthetic Minority Oversampling Technique(SMOTE) algorithm, which uses nearest neighbours to impute additional data points for the positive training example. In other words, SMOTE examines two nearby positive class examples and creates a new synthetic example in the middle of these two examples (see Appendix 5.3.3 for more details).

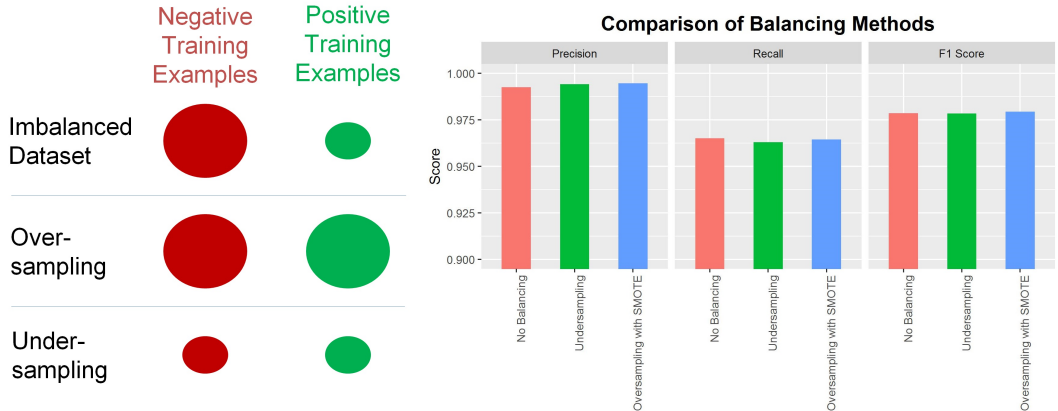


Figure 17: a) Graphical Illustration of Sample Balancing. b) Effect of Sample Balancing Techniques on Prediction Ability.

Interestingly, we note that overall, undersampling, oversampling and no sampling at all had very small effects on precision, recall and the final F1 score (Figure 17). Specifically, all three metrics were within a range of 0.003 for the different sampling techniques. We suspect that sample balancing did not significantly improve the performance because the synthetic dataset may have clearly separable positive and negative examples that would not benefit from any sampling.

However, we noted that oversampling techniques resulted in a marginally higher F1 score (0.001 higher than undersampling and no sampling), and because balanced datasets can minimise further bias in downstream analyses (Chawla, 2005), we used SMOTE oversampling to balance the training samples for all the network analysis.

### 3.6 Benchmarking of Optimised Network with the Synthetic Dataset

Following optimisation steps, we finalised the network architecture as similar to that in Figure 13, but with eight layers before the merge layer. We chose the Adam optimizer with a learning rate of  $10^{-5}$ . With this network configuration, we benchmarked the neural network against the single variant callers, as well as concordance callers, which are an integration of the outputs of the five variant callers. Specifically, the n-concordance variant caller is defined as the set of calls that any n callers agree upon – so 1-concordance includes all the calls made by all callers and 4-concordance includes all the calls made by any four callers.

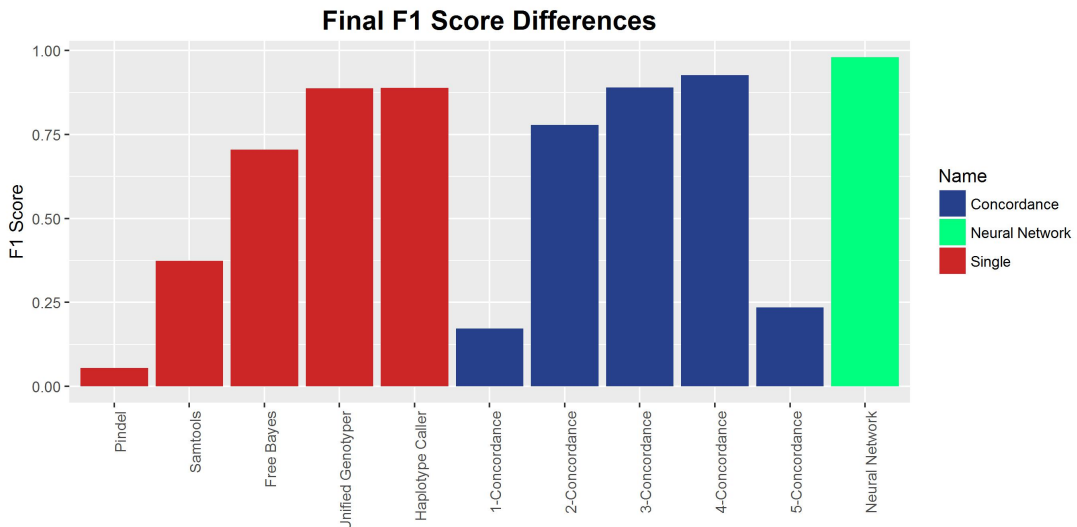


Figure 18: Overall Comparison of Variant Callers

Using the overall F1 score as the performance metric (Figure 18), we found that the neural network was able to outperform single and concordance-based callers. This provides strong evidence that the neural network can learn from the input features to identify high-confidence variant calls. The final F1 score obtained by the best single variant caller was the GATK Haplotype Caller at 0.888, and the best concordance caller had an F1 score of 0.927, while the neural network achieved the highest F1 score of 0.980. To gain insight into the improved accuracy, we examined the improvements in the precision and recall scores and found that the gain in the F1 score is due to the increased precision of the neural network, while the recall scores for different calling strategies were similar (Figure 19).

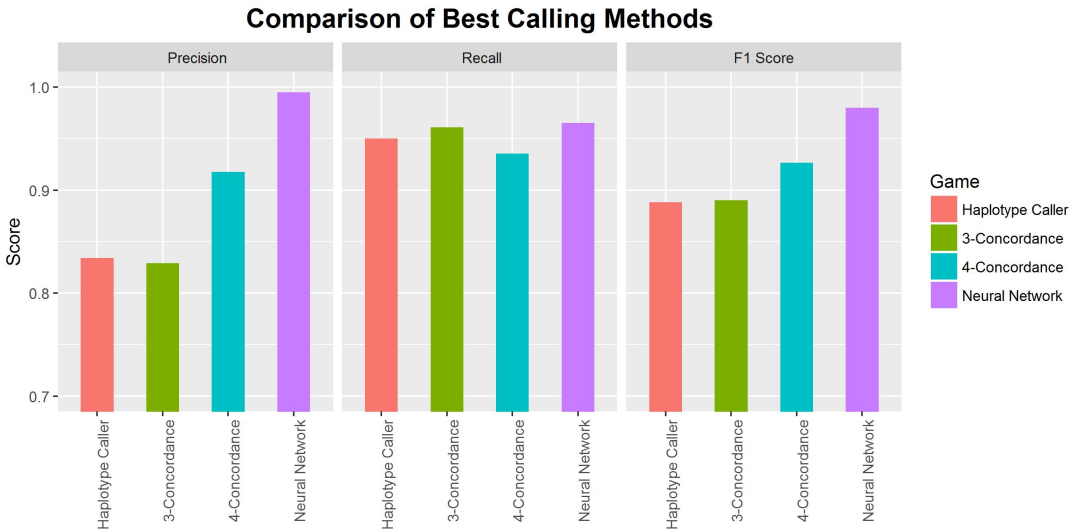


Figure 19: **Comparison of Best Variant Callers in terms of Precision, Recall and F1 Score**

Closer examination of the performance metrics revealed the neural network had the highest precision of 0.995 compared to only 0.917 for 4-concordance call. This represents a 20 fold decrease in the number of false positives or about 23,000 less false positive calls in the neural network compared to the four concordance caller. Interestingly, the recall of all the callers was high in the range of 0.90 to 0.95, indicating that while all callers were able to pick out most of the truth variant calls, the majority of the errors came from a high number of false positives.

In summary, the neural network had an F1 score that was 11% above the best single caller and 6% above the best concordance caller. Thus, this provides strong evidence that the neural network can sieve out false positives within the dataset and stably predict whether a mutation is true.

### 3.7 Benchmarking of Optimised Network with NA12878 Reference Dataset

After validation of the optimised neural network on the synthetic dataset, we next tested the performance of the neural network on a real dataset. To do this, we used the NA12878 Genome In a Bottle dataset (Zook et al., 2014), which has been used in other variant calling validation pipelines (Talwalkar et al., 2014; Linderman et al., 2014). This reference set contains a set of high-confidence variant calls which can be used as ground truth for training and validation. These high-confidence variant calls are obtained from multiple orthogonal sequencing methods

using Solid, Illumina, Roche 454, and Ion Torrent platforms. The intersection of the calls from these platforms was used to build a set of high-confidence variant calls.

Using this reference dataset, we evaluated the performance of our neural network and compared it to the single and concordance based variant callers. To do this, we applied the same pipeline to the NA12878 sequence reads as was done with the synthetic data.

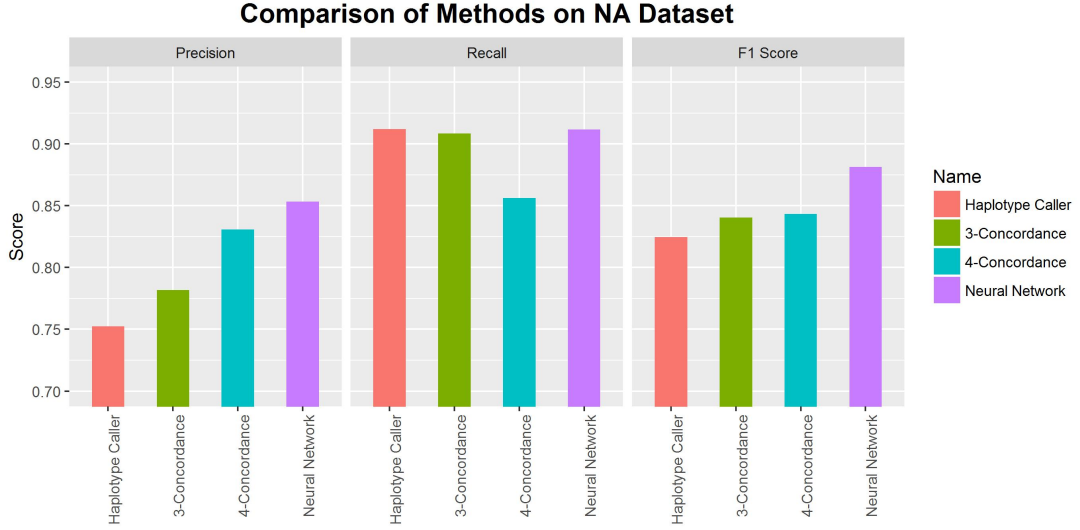


Figure 20: **Comparison of Variant Callers on NA12878 Dataset**

We found that the neural network was able to predict with the highest precision (0.859) when compared the best single caller, the GATK Haplotype Caller (0.752) and the two best concordance callers, 3-concordance (0.782) and 4-concordance (0.830) (Figure 20). For recall scores, the neural network had a higher recall rate (0.911) compared to the 4-concordance caller (0.856). Stated differently, the neural network was able to call 2650 more true variants and 1228 less false positives than the 4-concordance call set, indicating that the neural network was more aggressive in making variant calls, with a higher proportion of the calls being correct.

Finally, we found the neural network was able to outperform concordance variant callers by at least 4% and single callers by 6% in the F1 scores, supporting the notion that the neural network can significantly improve the calling of high-confidence variant calls for real datasets, in addition to synthetic ones.

### 3.8 Ranking of Functionally Important Mutations using a Bayesian Network

Because the number of variant/mutation calls can be large, we were motivated to develop a systematic approach to ranking the importance of functionally important mutations. This is done by combining the information about the confidence of a variant call from the deep learning network with functional annotations. To do this, we designed a Bayesian network that could evaluate the probabilistic scores for these events to compute a final likelihood of a functionally important mutation (Figure 21).

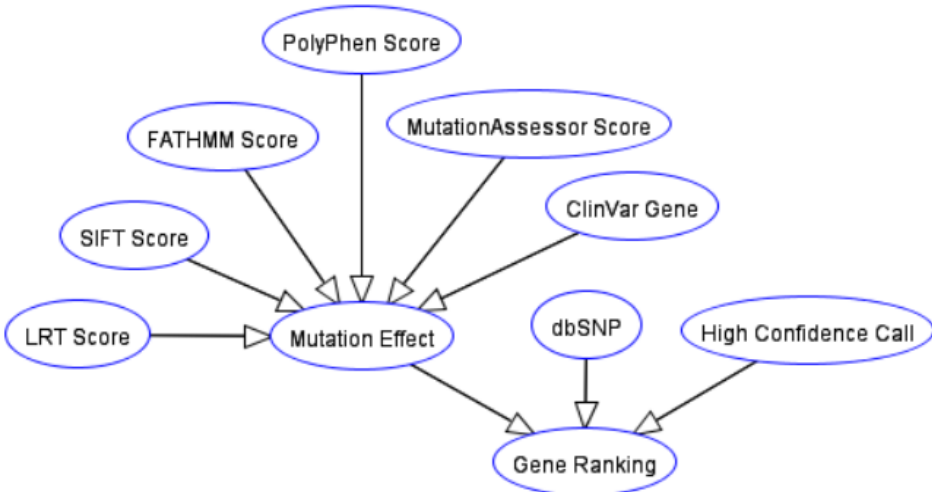


Figure 21: Final Bayesian Network used in Analysis

In this Bayesian network, we sought to integrate three different sets of probability scores to update the likelihood of the mutation being functionally important: (i) the probability of a high-confidence variant call; (ii) whether a variant is a common polymorphism; (iii) the probability of the mutation having a functional effect. This probability of a mutational effect is evaluated using information from ClinVar, a genotype-phenotype database (Landrum et al., 2014) and an ensemble of mutation effect predictors (Figure 21) that use statistical models to predict the effect of a mutation on protein structure and function. The annotations used in the network were obtained using ANNOVAR (Wang, Li, & Hakonarson, 2010) (Table 3).

Table 3: Functional Annotations obtained from ANNOVAR

Annotation Name	Information Type	Method	Scoring Method
Likelihood Ratio Test	Deleterious Mutation Score	Likelihood Ratio Test of each amino acid is evolving neutrally to the alternative model of evolution under negative selection	Score normalised to [0,1] and used directly in Bayesian Network
MutationAssessor	Deleterious Mutation Score	Mutation rate of homologous sequence subfamilies	Score normalised to [0,1] and used directly in Bayesian Network
SIFT	Deleterious Mutation Score	Position Specific Scoring Matrixes with conserved Sequences	Score normalised to [0,1] and used directly in Bayesian Network
PolyPhen2	Deleterious Mutation Score	naïve Bayes classifier on various multiple sequence alignments methods of homologous proteins and protein structure-based features	Score normalised to [0,1] and used directly in Bayesian Network
FATHMM	Deleterious Mutation Score	Hidden Markov Model used to score MSA based on protein homologous sequences	Score normalised to [0,1] and used directly in Bayesian Network
ClinVar Genes	Known Pathogenic Genes	Database lookup of curated set of relationship between variant calls and human phenotype	Higher Probability of Importance if known pathogenic variant
dbSNP138	Common Single Nucleotide Polymorphisms	Database lookup of curated set of known Human SNPs	Lower Probability of Importance if known common variant

Using this network, the likelihood of a functionally important mutation can be computed based on the conditional probabilities of the different events in the network as shown in the equation below.

$$P(Impt | (Func\ Eff \cap Rare \cap High\ Conf)) = \frac{P(Impt \cap Func\ Eff \cap Rare \cap High\ Conf)}{P(Func\ Eff \cap Rare \cap High\ Conf)} \quad (3)$$

$P(Impt)$  refers to the probability of the gene being important,

$P(Func\ Eff)$  refers to the probability of the gene having a functional effect,

$P(Rare)$  refers to the probability of the gene being uncommon and

$P(High\ Conf)$  refers to the probability of the gene being a high confidence call.

Intuitively, the probabilities of the different events are used to update the final likelihood of a functionally important mutation. For example, if the mutation was a common polymorphism, the likelihood of it being a disease-causing mutation would be less likely (Schork et al., 2009). Similarly, if a mutation was predicted to be a functional impact of a gene, the likelihood of it being a functionally important mutation would increase.

### 3.9 Validation of Bayesian Network Ranking of Mutations in a Patient-Derived Xenograft Cancer Model

To evaluate the effectiveness of our deep learning and Bayesian network ranking system, we analysed sequence reads from patient-derived xenograft (PDX) of a diffuse large B-Cell lymphoma (DLBCL), a cancer model with a well-defined disease progression (Knudson et al., 2001; Alizadeh et al., 2000). The PDX model would allow us to study the tumour in an *in vivo* envi-

ronment that permits longer term functional testing of candidate targeted therapies identified from mutation profiling (Tentler et al., 2012).

The sequence reads from the PDX DLBCL sample were analysed using the analysis pipeline that (i) identified high confidence variant calls by the deep learning network and (ii) ranked the functionally important mutations using the Bayesian network. The mutations were ranked by a Bayesian score indicating the probability of a high confidence mutation all that is functionally important (Figure 22).

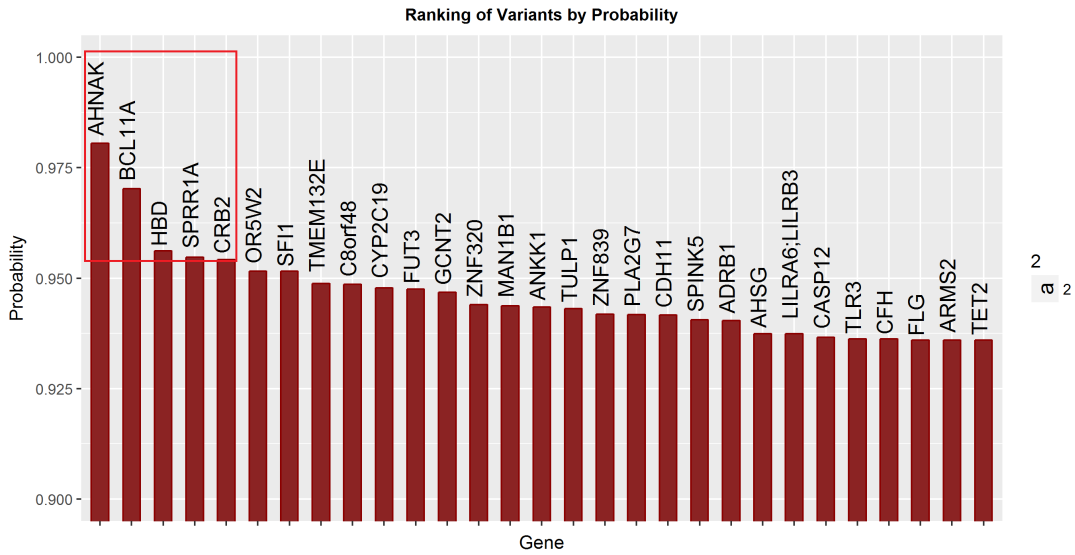


Figure 22: Top 30 genes from Bayesian Ranking Algorithm

Of the top 5 ranked mutations, we found that four of these five mutations were found in genes that have been implicated in lymphomas or other cancers (Table 4). AHNAK is a known tumour suppressor and has been known to be downregulated in lines of Burkitt Lymphoma (Lee et al., 2014; Amagai et al., 2004; Shtivelman et al., 1992). BCL11A is a known proto-oncogene in DLBCL and has been found to be overexpressed in 75% of primary mediastinal B-cell Lymphomas, a subset of DLBCL (Weniger et al., 2006; Satterwhite et al., 2001). SPRR1A, the fourth gene ranked in terms of importance, has been shown to be expressed in DLBCL (Zhang et al., 2014) and its expression has been shown to strongly correlate with 5-year survival rate (Figure 23). Finally, development of B-cell lymphoma has been noted in CRB2 related syndrome, which is a bi-allelic mutation of CRB2 (Slavotinek, 2016; Lamont et al., 2016). Interestingly, one of the top 5 ranked mutations was linked to a subunit of haemoglobin. While there is no strong evidence for the role of Haemoglobin in DLBCL, it has been shown to be expressed in aggressive glioblastomas lines, indicating a possible previously unknown role in

cancer (Emara et al., 2014).

Our findings suggest that the Bayesian network analysis can identify functionally important mutations in highly relevant genes. This ranking would help prioritise mutations in relevant genes among a large number of mutations identified by the variant caller that would have been difficult to evaluate without a systematic analysis.

Table 4: Highest Ranked Genes from Bayesian Ranking

Gene	Full Name	Known Involvement in Lymphoma or Cancer	Evidence	Mutation Location	Predicted Mutation Type
AHNAK	Neuroblast Differentiation-Associated Protein (Desmoyokin)	<ul style="list-style-type: none"> <li>Known <b>tumour suppressor</b> via modulation of TGF<math>\beta</math>/Smad signalling pathway</li> <li>Known to be <b>downregulated</b> in cell lines of Burkitt lymphomas</li> </ul>	Lee et al., 2014; Amagai et al., 2004; Shtivelman et al., 1992	chr11 - 62293433 T -> C	non synonymous SNV
BCL11A	B-Cell CLL/Lymphoma 11A	<ul style="list-style-type: none"> <li>Known proto-oncogene in DLBCL</li> <li>Overexpression of BCL11A was found in 75% of primary mediastinal B-cell lymphomas (a subset of DLBCLs)</li> </ul>	Weniger et al., 2006; Schlegelberger et al. 2001; Satterwhite et al., 2001	chr2 - 60688580 C -> G	non synonymous SNV
HBD	Hemoglobin Subunit Delta	<ul style="list-style-type: none"> <li>Shown to be <b>expressed</b> by aggressive glioblastoma cell lines</li> </ul>	Allalunis-Turner et al., 2013	chr11 - 5255274 G -> A	stop-gain
SPRR1A	Small Proline Rich Protein 1A (Cornifin-A)	<ul style="list-style-type: none"> <li>Known to be <b>expressed</b> in DLBCL and expression has been shown to correlate with 5 year survival rate</li> </ul>	Liu et al., 2014	chr1 - 152957961 G -> C	non synonymous SNV
CRB2	Crumbs 2, Cell Polarity Complex Component	<ul style="list-style-type: none"> <li>Cell polarity and cytoskeletal reorganisation is known to affect B-cell lymphoma migration and invasiveness</li> <li>Development of B-cell lymphoma has also been noted in Crb2-related syndrome (bi-allelic mutation of Crb2)</li> </ul>	Slavotinek, 2015; Gold et al., 2010	chr9 - 126135887 T -> C	non synonymous SNV

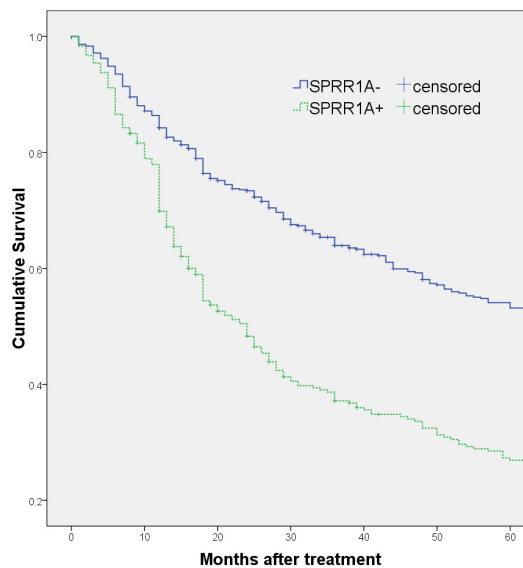
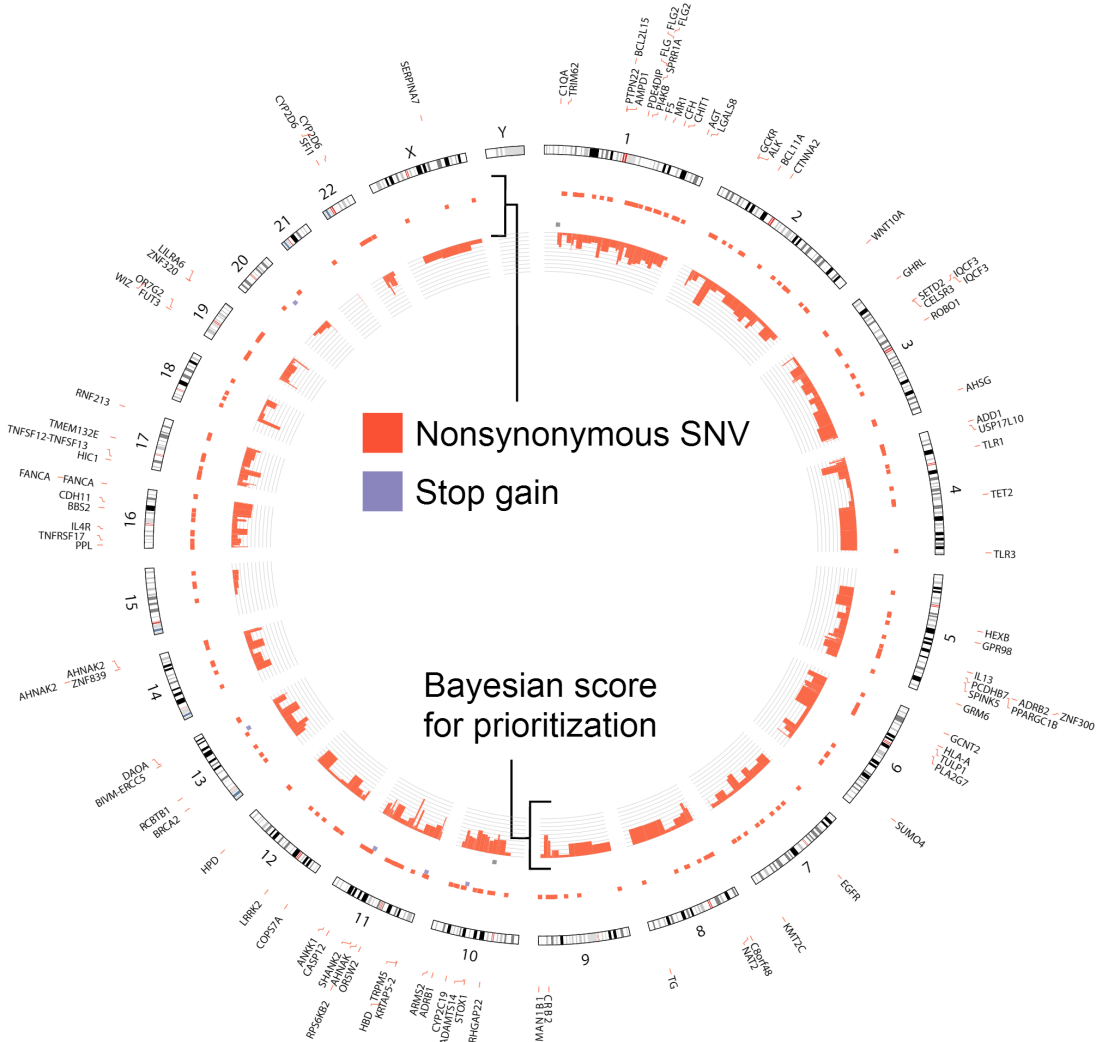


Figure 23: **5 Year Survival Curve of Patients with SPRR1A positive and SPRR1A negative DLBCL.** Patients that were SPRR1A positive were noted to have a significantly lower 5 year survival rate than patients that were SPRR1A negative. Source : Zhang et al. (2014), Figure 2.

To visualise the ranking of mutations from the Bayesian network, we plot the mutations

and the Bayesian scores using a Circos plot (Figure 24).



**Figure 24: Circos Plot of Top 100 Ranked Genes from Bayesian Network Ranking.** In this Circos plot, the outer track indicates the top ranked genes and their positions on the chromosome. The inner track describes the type of mutation that was observed – most mutations were non-synonymous SNVs, with a few stop-gain mutations. The innermost track shows the relative probabilities of each ranked gene.

Of the top 100 mutations (Figure 24), we identified several other gene families of possible relevance to B-cell lymphoma. These include several Toll-Like Receptors(TLRs), TLR3 (chr4,rank 26) and TLR1(chr4,rank 77) as well as interleukin receptors IL4R (chr16,rank 37) and IL13 (chr5,rank 75). TLRs are of significant interest in DLBCL because to their interaction with MYD88 (Yu, Wang & Chen, 2012), which is a well-characterised oncogene in DLBCL (Kraan et al., 2013; Ngo et al., 2010). Interleukin receptors are also important in DLBCL due to their importance in mediating inflammation and immune response (Balkwill & Mantovani, 2001), which is known to be affected in DLBCL (Monti et al., 2005). Thus, we conclude that our

Bayesian network can identify highly relevant gene families that are implicated in lymphoma progression.

## 4 Discussion

In this study, we sought to address the two major problems that limit the use of next generation sequencing in clinical genomics: (i) the identification of high-confidence variant calls; and (ii) the ranking of functionally important genes.

We demonstrate the validation of high-confidence variant calls using an optimised deep learning neural network on both real and synthetic datasets, and we also show that a Bayesian network can rank and prioritise genes in a systematic way so as to obtain functionally important genes. Consistent with the validity of our approach, we show that four of the top five genes had published findings that linked them with B-Cell lymphoma. Of the top 300 genes ranked, we also found families of genes that are known to be involved in lymphoma progression, including the Toll-like receptor and interleukin receptor families.

### 4.1 Adapting Deep Learning for Improving Variant Calling Accuracy

Deep learning networks have been used successfully to solve complex non-linear problems, including performing facial recognition (Sun et al., 2014) and predicting drug molecule solubility (Lusci et al., 2013). In this study, we demonstrate that a deep learning architecture can be used to integrate complex features from an ensemble of variant callers to improve variant calling accuracy. We found that not all network architectures were suitable for processing the complex features. When a typical flat network architecture was used, the network was unable to converge and learn, suggesting that the number of features was too high for optimal learning. Interestingly, when the number of features was compressed using PCA, a commonly used dimensionality reduction algorithm, the flat network was still unable to learn, indicating that compression of features did not play a major role in the improving the performance of flat networks.

Because the straightforward application of flat networks did not work well, we reasoned that the complex features from each variant caller represented multimodal data and a merged architecture would be more suitable to learn from such a feature set (Eitel, 2015; Suk, Lee & Shen, 2014). Consistent with this hypothesis, we developed a merged network architecture that comprised of subnets for features of each variant caller that were subsequently merged into a common network for variant call prediction.

When the merged architecture network was further optimized by varying the network layers, gradient descent optimizers and sample balancing, we did not observe any significant improvements in the variant calling performance, suggesting that the merged architecture for multimodal data was the most significant contributor to the ability of the network to learn from an ensemble of variant callers.

Using our optimised merged network architecture, we were able to call variants more accurately than single or concordant variant callers, with F1 score improvements of 6% in synthetic datasets and 4.5% in the NA12878 dataset. Although several ensemble methods have been proposed such as VariantMetaCaller and BAYSIC (Gézsi et al., 2015; Cantarel et al., 2014), the performance metrics reported were not directly comparable to the F1 scores used in this study. It would be of interest to implement a pipeline with all the ensemble methods in a common framework to enable proper comparisons of the variant calling performance.

## 4.2 Improving Performance of Deep Learning Approach

Although the deep learning network was able to improve the accuracy of variant calling, there are several areas worth looking into that would likely improve their performance. These areas include increasing the number of input features, as well as generating real-world datasets with established ground truth variant calls.

Firstly, deep learning networks, like any machine learning algorithm, are highly dependent on the features used in the input layers for pattern identification and prediction. In our study, we chose five variant callers that are commonly used and correspondingly the feature set is limited by the outputs provided by each variant calling algorithm. The inclusion of other orthogonal features from alternative variant callers and alignment tools may provide additional data that can improve prediction accuracy.

Secondly, the accuracy of the deep learning network is also highly dependent on the training datasets. In this study, we trained the optimised network using the NA12878 dataset which includes a set of high confidence calls from the integration of calls from several orthogonal sequencing technologies. However, as the ground truth calls in the NA12878 are also subjected to noise and biases from sequencing, it is likely that some ground truth calls may have been misclassified, leading to false positive and false negative calls. Indeed, Zook et al.(2014) esti-

mate a possible false negative or positive for every 30 million bases in the NA12878 dataset. To address this problem, several ongoing efforts are focused on obtaining verified truth variants by Sanger sequencing, which remains the gold standard for identifying prevalent mutations (Tsiatis et al., 2014). The establishing of verified variants would provide a training set that would be a major step in improving the accuracy and performance of a deep learning network.

### 4.3 Improvements to Bayesian Network

In this study, we used a Bayesian model to rank important genes from a DLBCL sample. Encouragingly, we found that four of the five top-ranked mutations were linked to B-Cell lymphoma, indicating that the validity of a Bayesian network approach to identify functionally important genes. Furthermore, we were able to find important receptor families known to be clinically relevant in DLBCL, such as the Toll-like receptor (Yu, Wang & Chen, 2012) and interleukin receptor families (Monti et al., 2005; Balkwill & Mantovani, 2001), providing further evidence for the use of Bayesian networks in gene prioritisation.

However, one key limitation in such a Bayesian network is the setting of prior probabilities and conditional probabilities for the network. In the design of the Bayesian network, we had to make assumptions regarding the prior and conditional probabilities - for example, we set the probability of a gene being important if it is a common polymorphism as 0.3, and 0.7 if it is not a common polymorphism. These assumptions are necessary as because it is difficult to obtain the true probabilities - in the same example, trying to find the probability it is important would entail finding out all common polymorphisms and then aggregating each polymorphism's probability of having a phenotypic effect. A possible way around this issue is to engage a panel of experts to provide input on the prior and conditional probabilities. This technique has been used to build Bayesian networks in other fields including risk assessment and ecology (Lee, Park & Shin, 2009; Uusitalo, 2007), and is useful when the true prior and conditional probabilities are difficult to observe. This method relies on the expert's causal understanding of the interactions between the observations and the outcomes and has been shown to be a relatively good approximation to provide the conditional and prior probabilistic relationships (Choy, O'Leary & Mengersen, 2009).

A second limitation with our current network structure is the equal ranking of mutation effect, the prevalence of the SNV and the confidence of a variant call. With this network structure, a

high confidence mutation that is not functionally important could be prioritised over a lower confidence but more functionally important mutation. Since we are chiefly concerned with the mutation’s functional importance, this network structure might not be the most suitable for prioritising the most important genes. One potential improvement is to study how the hierarchy can be altered - specifically to see if the high-confidence node could be used as a prior probability to all the other nodes, which makes more intuitive sense and reduces its importance in the overall network.

One final limitation of the Bayesian network is the lack of a gold standard to benchmark its ranking ability. In deep learning, we were able to validate our results using synthetic datasets and the NA12878 dataset – while these are not perfect standards, they could still be used for preliminary validation. However, for the Bayesian network ranking, we can only infer the validity of such a method by looking at approximate measures, such as how many of the top ranked genes were linked to DLBCL. To properly test such a ranking system, a sample has to be obtained where the key driver mutations well-characterised by other techniques and methods. Thus, one possible extension of this project is to perform ranking on a disease sample where the key driver mutations have already been determined and elucidated via other techniques, and verifying to see if the ranking system can prioritise those genes.

#### 4.4 Clinical Usage of Bayesian Networks in Gene Prioritisation

We specifically chose the Bayesian Network structure as it presents a clear and understandable predictive model that clinicians can use in a clinical setting. Compared with other genomic-based tools being currently used now like gene panels (Olek and Berlin, 2002), Bayesian Networks have the added advantage of not being limited to a specific set of genes. This allows doctors to find other similar proteins or interacting agents that might be related to the known deleterious genes and use that information in their treatment and diagnosis (Meldrum et al., 2011).

However, one limitation in implementing such a Bayesian network in the clinic is that all the information that goes into it has to be manually curated. Because it taps upon previously curated databases, it is limited in scope to the pre-processed information it already contains,

and effort has to be spent to update these databases when new findings emerge. One possible alternative to solve this problem is to develop a data miner to mine the literature for possible relationships between genes and diseases, thus creating a self-updating database. However, this is currently difficult to implement because a machine would have to learn the complex conceptual relationships between genes and phenotype, and this is currently an unsolved problem (Cambria & White, 2014). Furthermore, such a system would require still human intervention to verify the data being mined is valid and appropriate. Ultimately, the current implementation should still be a useful tool as it allows for an interface for clinicians and researchers to easily share and obtain information, and a single clinician to tap on the expertise and data from many different research institutions without having to sieve through the literature manually.

## 4.5 Future Directions

There are several avenues that the integrated deep learning and Bayesian network analysis could be extended to improve the performance and utility.

1. To improve the performance of the deep learning network, additional features from other variant callers could be included in the pipeline to provide more orthogonal data for prediction accuracy. Also, the network could be trained on additional real datasets with ground truth variant calls so that the network can generalise and predict high-confidence variant calls on a wide range of datasets.
2. The Bayesian network could be extended to integrate information about druggable gene and variants using a drug-gene interaction database such as DGldb (Griffith et al., 2013). This would enable the prioritisation of mutations which have possible candidate drug targets.

## 4.6 Conclusion

In this study, we have shown the use of deep learning neural networks to validate variants in both real and synthetic datasets successfully. We also show that using a Bayesian network can identify important genes within a lymphoma disease sample. Ultimately, we hope to be able to put these networks to use in a clinical setting to augment treatment and diagnosis of diseases.

## 5 Appendixes

### 5.1 Neural Network Learning

Machine learning with deep neural networks is underpinned by two key phases, the feed-forward phase and the backpropagation phase.

#### 5.1.1 Feedforward Phase

The feedforward phase describes the computation of a prediction, and during this phase, the input features are used to compute the final output prediction. For a simple network below:

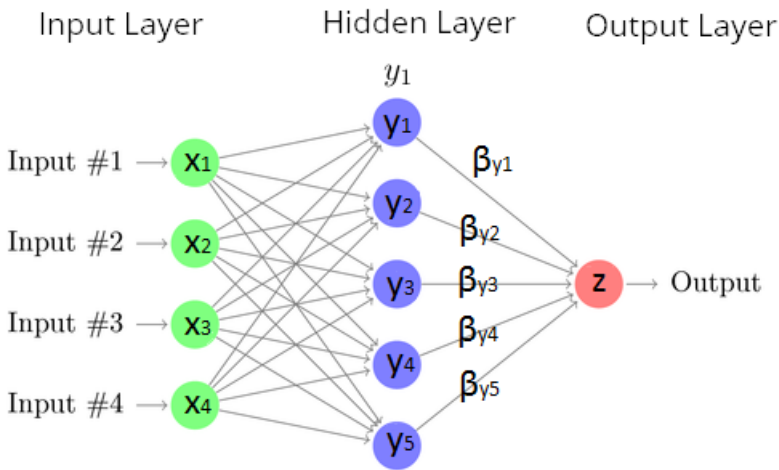


Figure 25: Sample Neural Networks with Labelled Nodes and Weights.

The final prediction,  $z$  is computed with the equation:

$$z = \beta_{y1} * y_1 + \beta_{y2} * y_2 + \beta_{y3} * y_3 + \beta_{y4} * y_4 + \beta_{y5} * y_5 \quad (4)$$

Where  $\beta$  indicates, the weights linking each output to the input of  $z$  and each of the  $y_i$  terms are computed in the same manner from the  $x_i$  layer. At each node  $(x,y,z)$ , there is also the existence of an activation function that modifies the input of the node to compute an output. Commonly used activation functions include the rectified linear unit (ReLU), sigmoid functions like hyperbolic tangent and logistic function,  $S(T) = \frac{1}{1+e^{-T}}$ . Thus, the final prediction can be seen as a summation of all weights multiplied by the activation output of each node. In theory, we can expand each of the  $y_i$  terms in equation (2) to include the  $y_i$  layer activation function as well as rewrite the  $y_i$  layer inputs in terms of the sum of outputs and weights from the  $x_i$  layers. This complex integration of terms allows for the neural network to form complex

continuous decision boundaries as the neural networks can compute sophisticated non-linear prediction functions despite being a fundamentally linear model.

### 5.1.2 Backpropagation Phase

After a prediction is made, we then have to check whether it is correct and change our weights if an erroneous prediction was made (Figure 26).

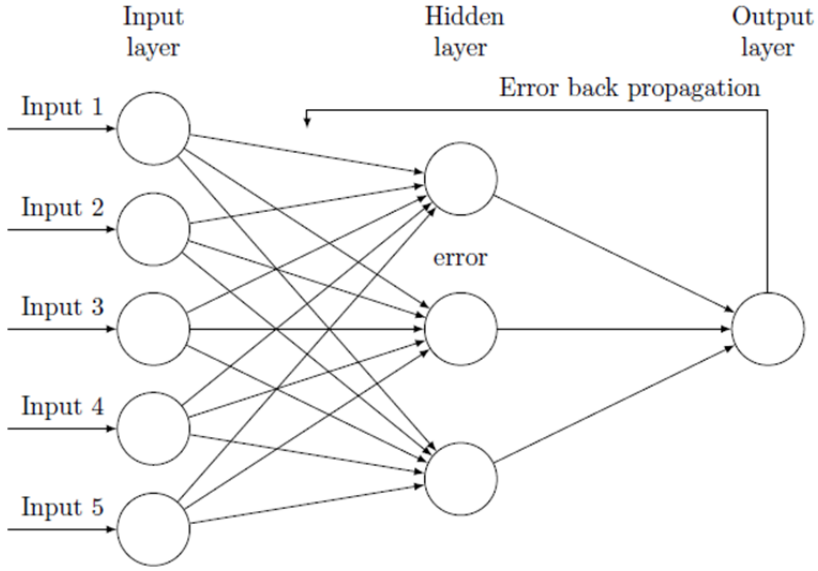


Figure 26: Backpropagation of Error Terms

This is the backpropagation step, which involves backpropagating the error terms from the output layers to the input layer and updating the weights at each node based on the differential relationship between the error and each specific gradient. Specifically, this is governed by the optimiser functions which have been mentioned earlier – one example of such a function is the Stochastic Gradient Descent function, which is

$$\beta_{yi}^n = \beta_{yi}^{n-1} - \alpha \frac{\partial E_n(\beta)}{\partial \beta_i} \quad (5)$$

Here, each  $\beta$  term indicates a gradient,  $\alpha$  is a constant for the learning rate and  $\frac{\partial E_n(\beta)}{\partial \beta_i}$  is the term used to modify the weight of the gradient based on the cost function  $E_n(\beta)$ . The idea used in all backpropagation functions is gradient descent, where the contribution of the gradient term to the error is computed, and the gradient is changed by an amount in order to reduce the future contribution of the gradient to that error.

### 5.1.3 Cost Function in Gradient Descent

Here it is useful to consider what the cost function  $E_n(\beta)$  is. It is essentially the error rate when a set of gradients is used to perform predictions, as it measures how many accurate predictions were made and how many wrong predictions were made. For a binary class predictor (which is what we are using, only true and false), this is given by the equation

$$E(\beta) = -\frac{1}{n} \sum_{i=1}^n \sum_{j=1}^2 y_{ij} \log(p_{ij}) \quad (6)$$

where  $y_{ij}$  indicates the empirically observed probabilities of each class label while  $\log(p_{ij})$  is the theoretical probabilities of each class label. This is also known as binary cross-entropy, which is derived from Shannon's entropy (See Appendix 5.2.1). From this term, we see that if the neural network predicts something with a high probability ( $y_{ij}$  is high) and it is false ( $p_{ij}$  is low) so then  $\log(p_{ij})$  is a big negative number, and so the cost function will very high. On the other hand, if  $y_{ij}$  and  $p_{ij}$  is high then the entropy will be close to zero, indicating a correct prediction. Since each of the prediction terms can be rewritten in terms of the gradient (rewrite  $z$  in terms  $\beta y_i$  and so on), we can theoretically compute the contribution of each gradient to the cost function to see how the cost function changes as the gradient changes. Thus, this is what gradient descent does – it tries to see how the cost function changes as each gradient changes, then attempts to move the gradient in the direction that minimises the error term.

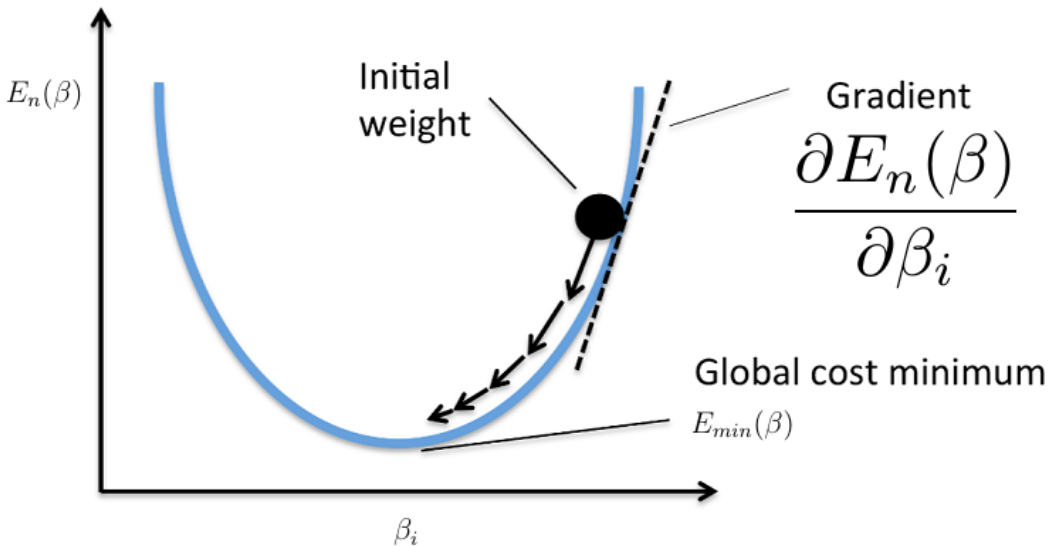


Figure 27: **Graphical Illustration of Gradient Descent.** Gradient descent attempts to find the gradient at which the cost function is minimised (since the cost function depends on the gradient).

This is best seen in Figure 27 above, where the gradient or specifically the partial differentiation of the cost function with regards to each gradient is used to move the gradient to a new position so as to minimise the error term. Thus, machine learning is, in essence, a minimisation problem – we want to find a set of weights that minimises the cost function. Because the cost function describes how many predictions we made correctly, gradient descent essentially trains our network to accurately predict outputs from inputs.

## 5.2 Feature Engineering

We subset our features into three broad sets, which are base-specific information, sequencing error and bias information features, and calling and mapping quality. Base information tells us base specific properties, including information contained in the base as well as the quality of sequenced bases in the samples. Sequencing error and bias features attempt to tease out potential biases in sequencing, including features such as GC content, longest homopolymer run and as well as allele balances and counts. Finally, calling and mapping quality provides information on the mapping and calling confidence of the variant callers, and includes features such as genotype confidence and mapping quality. In all, these sets of information provide information on the key aspects of variant calling – specifically the properties of the bases in the samples, the characteristics of the sequencing process and finally the variant calling and mapping algorithms.

### 5.2.1 Base Information

#### Shannon Entropy

Shannon Entropy captures the amount of information contained in the allele sequences. It is calculated using the equation:

$$H(X) = - \sum_{i=1}^n P(x_i) \log_2 P(x_i) \quad (7)$$

where  $P(x_i)$  is the probability of finding each base at each position. Thus, we calculate the entropy by summing up the probabilities/ $\log(\text{probabilities})$  at each position. This prior probability is calculated in two ways, and both are used as features – firstly, the overall genome base probabilities are calculated over the entire genome, and thus the entropy is related to the probability of finding a base at any position in the genome. The second way prior probability is calculated is to take a region of space around the allele (10 bases plus the length of the allele in our calculations) and use those probabilities to calculate the entropy of the allelic sequence. Intuitively, it attempts to find out the amount of information contained within the allelic sequence, and hopefully, the neural network can use the information to determine the validity of a mutation.

### Kullback Leibler Divergence

The Kullback-Leibler Divergence feature is similar to Shannon entropy, but instead, we use this to measure the informational change converting from the reference to the allele sequence.

The Kullback-Leibler Divergence is calculated as follows:

$$D_{KL}(P||Q) = - \sum_{i=1}^n P(x_i) \log_2 \frac{P(x_i)}{Q(x_i)} \quad (8)$$

where  $Q(x_i)$  is the prior probability of finding each base at each position based on the genomic region around the allele, while  $P(X_i)$  is the posterior probability of finding a specific base inside the allelic sequence. Thus, the KL divergence describes the informational gain when the probabilities from Q are used to describe P. Intuitively, since we know the base probabilities of the region, we can then study the probabilities observed in the reference allelic sequence and see how well  $Q(X_i)$  probabilities can approximate  $P(X_i)$  probabilities.

### Base Quality

Base quality refers to the Phred score probability that the called allele is wrong. It is given by the equation:

$$P = 10^{-\frac{Q}{10}}$$

Where P is the Base Quality, and Q is the probability that the allele called is wrong. This is a number computed by the sequencing machine based on the quality of the base samples provided, and tells us how much confidence the sequencing machine has in calling that base.

### **5.2.2 Sequencing Biases and Errors**

#### GC content

This feature computes the calculated GC content of reference genome, which may affect sequencing results and accuracy as regions with a GC content are known to be more difficult to sequence. This is because of the greater strength of GC bonds, resulting in errors and biases in sequencing (Benjamini & Speed, 2012).

#### Longest homozygous run

Homopolymer runs (AAAAAAA) are known to cause sequencer errors (Quail et al.,2012),

and might be a factor in determining whether a variant is true. This because long homopolymers provide the same type of signal to the sequencing machine, resulting in a difficult in estimating the magnitude of the signal or rather how many bases are in that homopolymer, resulting in errors and wrongly called variants. The reference sequence region including the allele was checked for homopolymer runs.

#### Allele Count

Allele count gives the total number of alleles in called phenotypes. This feature provides information of possible biases in the sequencing machine.

#### Allele Balance

Allele Balance describes the ratio of final allele called over all other alleles called(reference allele for heterozygous calls, or other alleles for homozygous calls). This feature give us information of possible biases in the sequencing machine.

#### Allele Frequency

Allele Frequency describes the ratio of final allele called over all other alleles called(reference allele for heterozygous calls, or other alleles for homozygous calls). This feature give us information of possible biases in the sequencing machine.

### **5.2.3 Calling and Mapping Qualities**

#### Genotype Likelihood

The genotype likelihood provides the Phred-scaled likelihood scores of how confident the caller is in determining that it is a homozygous or heterozygous call, and for the homozygous calls whether it is a more likely to be a bi-allelic mutation or no mutation at all. This feature thus gives us the confidence of the caller in determining if one or two alleles have mutated.

#### Read Depth

Mapped read depth refers to the number of bases sequenced and aligned at a given reference base position. The read depth tells us how many reads contributed to a specific call, and thus provides information on how much evidence there is for the variant call

### Read Depth, 4 Variables

This feature is a refinement of Read Depth, and provides 4 variables for the number of forward reference alleles, the number of reverse reference alleles, the number of forward non-ref alleles and finally the number of reverse non-reference alleles.

### Allele Depth

This feature is a refinement of Read Depth, and describes the number of alleles supporting the variant call.

### Quality by Depth

Quality by Depth is computed by dividing the quality score against allele depth, to obtain an average score of allele quality. This composite feature provides information on the information provided by each read supporting the call

### Mapping Quality

Mapping quality is originally a score provided by the alignment method and gives the probability that a read is placed accurately. The variant callers compute an overall mapping quality of the reads that provide evidence for a variant call which is given in this feature. A low mapping quality means that there are multiple positions where the reads contributing to this variant call could have gone, and thus providing evidence that this might not be an accurate call due to poor mapping.

### Mapping Quality of Observed Reference Alleles

This feature is a refinement of Mapping Quality, and describes the mapping quality of observed reference alleles.

### Mapping Quality of Observed Alternate Alleles

This feature is a refinement of Mapping Quality, and describes the mapping quality of observed alternate alleles.

## 5.3 Mathematical and Statistical Tools

### 5.3.1 Derivation of F1 Score

The F1 score is a useful measure as it can measure both the precision as well as the recall of a predictor. For a binary predictor with a binary truth class(Figure 28), we can obtain four types of results – true positives, true negatives, false positives and false negatives.

		Predicted Class	
		Yes	No
Actual Class	Yes	True Positive	False Negative
	No	False Positive	True Negative

Figure 28: Confusion Matrix for a Binary Class Predictor.

True positives are positive predictions that are made that are positive class labels, while false positives are positive predictions that are made that have negative class labels. Similarly, true negatives are negative predictions that have negative class labels, while false negatives are negative predictions that are positive class labels. From this, we can define two equations, precision and recall. Precision is defined as (8) while recall is defined as (9).

$$Precision = \frac{True\ Positive}{True\ Positive + False\ Positive} \quad (9)$$

$$Recall = \frac{True\ Positive}{True\ Positive + False\ Negative} \quad (10)$$

Precision tells us how likely a positive prediction made will be true, while recall tells us how much of the truth class positive predictions the predictor can classify successfully . Thus, a predictor can have a high precision but low recall (makes few predictions but are very accurate) or a high recall and low precision(makes many predictions that capture all truth variables, but have a lot of false positives as well). In genomics, both types of errors are not desired – we would want all the predictions to be true (precision), while not losing out on any important mutations (recall). Thus, we use the composite metric, the F1 score, that looks at the overall

precision and recall of a predictor. It is defined as follows:

$$F1\ Score = \frac{2 * Precision * Recall}{Precision + Recall} \quad (11)$$

### 5.3.2 Principal Components Analysis (PCA)

Principal Components Analysis (PCA) is a commonly used tool for dimensionality reduction. It was first proposed by Pearson in 1901 (Pearson, 1901) and has been commonplace in many data analytics and signal processing methodologies (Jolliffe, 2002). PCA works by attempting to discover orthogonal principal components (PCs) that are able to represent the original data. Specifically, this means that the PCs can capture variance in the datasets. This is done by finding the Eigenvalues and Eigenvectors of the dataset, with the eigenvectors representing a linear combination of all input variables and the eigenvalues representing the amount of variance that that eigenvector can represent. Ultimately, we select n eigenvectors that can represent a percentage of variance in our dataset. Because each eigenvector is orthogonal, they can capture the variance in the dataset.

For our analysis, we decided to use eight principal components – we took the limit as the last principal component that was able to represent at least 0.5% of the variance in the dataset (Figure 29).

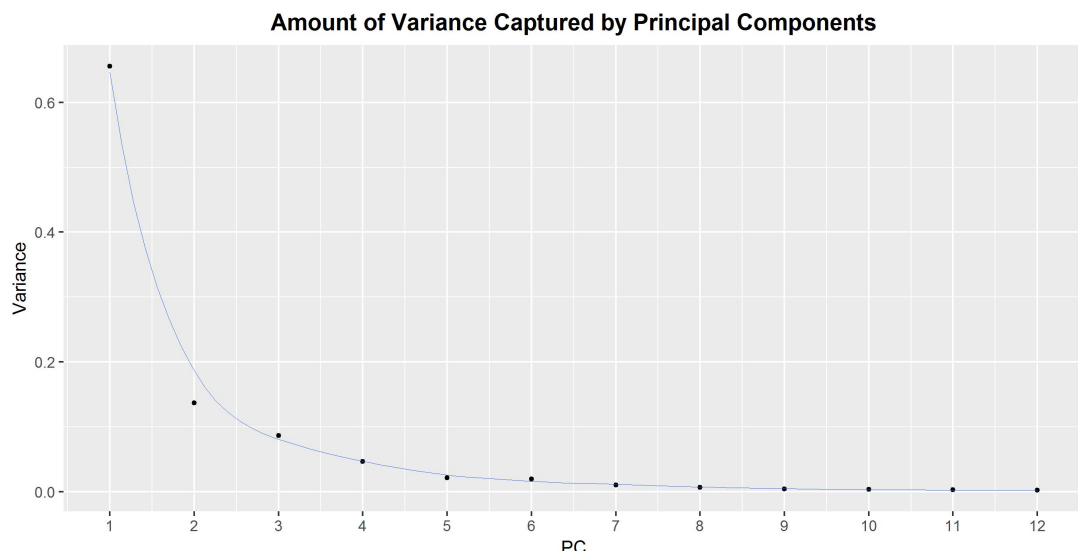


Figure 29: Variance Captured by First 12 Principal Components

To carry out PCA, we used the preprocessing step SciPy to normalise all the input vectors to mean 0 and standard deviation 1. Subsequently, we perform principal components decomposition to obtain the eigenvector transformed representation of the dataset and their corresponding eigenvalues. We then fit 8 of the principal components that explained the largest amount of variance into the neural network to study if it can learn from the compressed representation of the input features.

### 5.3.3 Synthetic Minority Overrepresentation Technique (SMOTE)

SMOTE is a statistical technique described in by Chawla et al. (2002) to overcome problems with imbalanced datasets that are common in machine learning. SMOTE oversamples the training class with fewer variables in a way that tries not to replicate data points (that makes certain data points over-represented) without creating new invalid training examples. It does this by taking the intersection of two nearest data points of the same training class. This can be seen in Figure 30.

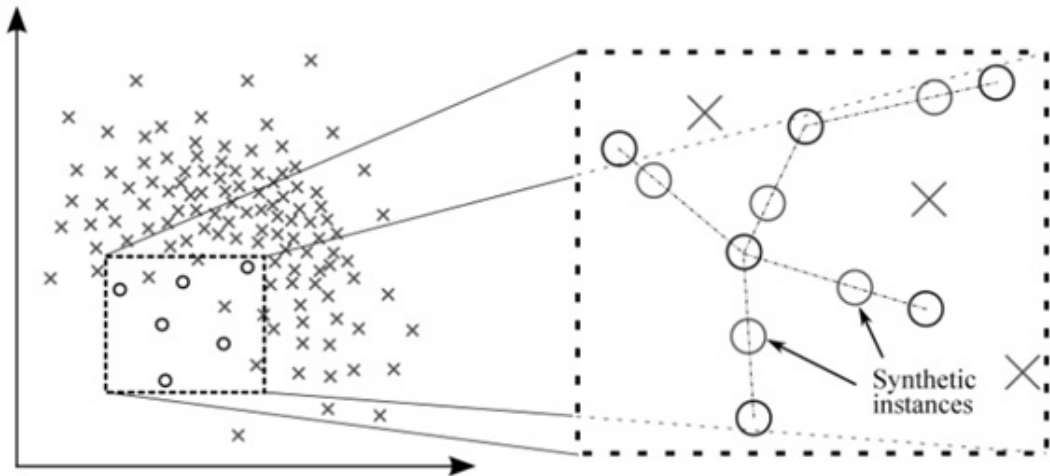


Figure 30: **Illustration of SMOTE Oversampling Algorithm.** Note the use of 2 nearest neighbours to create a new synthetic example. Figure from Chawla et al., 2002

In doing so, it creates a more generalised representation of the sample class with less training examples, without replicating certain datapoints and without creating invalid data. This enables intelligent oversampling of the dataset to balance out the positive and negative feature classes. SMOTE has been shown to be valid for other datasets including sentence boundary detection (Liu et al., 2006) and data mining (Chawla, 2005).

## 6 Bibilography

- Abeel, T., Van de Peer, Y., & Saeys, Y. (2009). Toward a gold standard for promoter prediction evaluation. *Bioinformatics* 25, i313-i320.
- Amagai, M. (2004). A mystery of AHNAK/desmoyokin still goes on. *Journal of investigative dermatology* 123, xiv.
- Abyzov, A., Li, S., Kim, D., Mohiyuddin, M., Stütz, A., Parrish, N., Mu, X., Clark, W., Chen, K., and Hurles, M. et al. (2015). Analysis of deletion breakpoints from 1,092 humans reveals details of mutation mechanisms. *Nature Communications* 6, 7256.
- Alizadeh, A., Eisen, M., Davis, E., Ma, C., Lossos, I., Rosenwald, A., Boldrick, J., Sabet, H., Tran, T., and Yu, X. (2017). Distinct types of diffuse large B-cell lymphoma identified by gene expression profiling. *Nature* 403, 503-511.
- Angrist, M. (2016). Personal genomics: Where are we now?. *Applied & translational genomics* 8, 1.
- Anthimopoulos, M., Christodoulidis, S., Ebner, L., Christe, A., & Mougiaakou, S. (2016). Lung pattern classification for interstitial lung diseases using a deep convolutional neural network. *IEEE transactions on medical imaging* 35, 1207-1216.
- Balkwill, F., & Mantovani, A. (2001). Inflammation and cancer: back to Virchow?. *The Lancet* 357, 539-545.
- Bengio, Y., Simard, P., & Frasconi, P. (1994). Learning long-term dependencies with gradient descent is difficult. *IEEE transactions on neural networks* 5, 157-166.
- Benjamini, Y., & Speed, T. P. (2012). Summarizing and correcting the GC content bias in high-throughput sequencing. *Nucleic acids research* 40.

Cambria, E., & White, B. (2014). Jumping NLP curves: a review of natural language processing research [review article]. *IEEE Computational Intelligence Magazine* 9, 48-57.

Chicago

Cantarel, B. L., Weaver, D., McNeill, N., Zhang, J., Mackey, A. J., & Reese, J. (2014). BAYSIC: a Bayesian method for combining sets of genome variants with improved specificity and sensitivity. *BMC bioinformatics* 15, 104.

Chawla, N. V. (2005). Data mining for imbalanced datasets: An overview. In *Data mining and knowledge discovery handbook* (pp. 853-867). Springer US.

Chawla, N. V., Bowyer, K. W., Hall, L. O., & Kegelmeyer, W. P. (2002). SMOTE: synthetic minority over-sampling technique. *Journal of Artificial Intelligence Research* 16, 321-357.

Chen, Y., Lin, Z., Zhao, X., Wang, G., & Gu, Y. (2014). Deep learning-based classification of hyperspectral data. *IEEE Journal of Selected topics in applied earth observations and remote sensing* 7, 2094-2107.

Choy, S. L., O'Leary, R., & Mengerson, K. (2009). Elicitation by design in ecology: using expert opinion to inform priors for Bayesian statistical models. *Ecology* 90, 265-277

CLC bio. (2011). Genomics Workbench User Manual 4.8. Finlandsgade 10-12 DK- 8200 Aarhus N, Denmark

Cornish, A., and Guda, C. (2015). A Comparison of Variant Calling Pipelines Using Genome in a Bottle as a Reference. *Biomed Research International* 2015, 1-11.

Cirulli, E. T., & Goldstein, D. B. (2010). Uncovering the roles of rare variants in common disease through whole-genome sequencing. *Nature Reviews Genetics* 11, 415-425.

Davis, J., & Goadrich, M. (2006, June). The relationship between Precision-Recall and ROC curves. In Proceedings of the 23rd international conference on Machine learning (pp. 233-240). ACM.

Danecek, P., Auton, A., Abecasis, G., Albers, C., Banks, E., DePristo, M., Handsaker, R., Lunter, G., Marth, G., and Sherry, S. et al. (2011). The variant call format and VCFtools. *Bioinformatics* 27, 2156-2158.

DePristo, M., Banks, E., Poplin, R., Garimella, K., Maguire, J., Hartl, C., Philippakis, A., del Angel, G., Rivas, M., and Hanna, M. et al. (2011). A framework for variation discovery and genotyping using next-generation DNA sequencing data. *Nature Genetics* 43, 491-498.

Di Tommaso, P., Chatzou, M., Baraja, P. P., & Notredame, C. (2014). A novel tool for highly scalable computational pipelines.

Egan, J. P. (1975). Signal detection theory and ROC analysis.

Eitel, A., Springenberg, J. T., Spinello, L., Riedmiller, M., & Burgard, W. (2015, September). Multimodal deep learning for robust rgb-d object recognition. In Intelligent Robots and Systems (IROS), 2015 IEEE/RSJ International Conference on (pp. 681-687). IEEE.

Emara, M., Turner, A. R., & Allalunis-Turner, J. (2014). Adult, embryonic and fetal hemoglobin are expressed in human glioblastoma cells. *International Journal of Oncology* 44, 514-520.

Escalona, M., Rocha, S., & Posada, D. (2016). A comparison of tools for the simulation of genomic next-generation sequencing data. *Nature Reviews Genetics* 17, 459-469.

Fawcett, T. (2006). An introduction to ROC analysis. *Pattern recognition letters* 27, 861-874.

Garrison, E., & Marth, G. (2012). Haplotype-based variant detection from short-read sequencing. arXiv preprint arXiv:1207.3907.

Gézsi, A., Bolgár, B., Marx, P., Sarkozy, P., Szalai, C., & Antal, P. (2015). VariantMetaCaller: automated fusion of variant calling pipelines for quantitative, precision-based filtering. BMC genomics 16, 1.

Griffith, M., Griffith, O., Coffman, A., Weible, J., McMichael, J., Spies, N., Koval, J., Das, I., Callaway, M., and Eldred, J. et al. (2013). DGIdb: mining the druggable genome. Nature Methods 10, 1209-1210.

Huval, B., Wang, T., Tandon, S., Kiske, J., Song, W., Pazhayampallil, J., Andriluka, M., Rajpurkar, P., Migimatsu, T., and Cheng-Yue, R. et al. (2017). An Empirical Evaluation of Deep Learning on Highway Driving. Arxiv 1504.01716.

Hwang, S., Kim, E., Lee, I., & Marcotte, E. M. (2015). Systematic comparison of variant calling pipelines using gold standard personal exome variants. Scientific reports 5, 17875.

Janitz, M. (Ed.). (2011). Next-generation genome sequencing: towards personalized medicine. John Wiley & Sons.

Jensen, F. V. (1996). An introduction to Bayesian networks (Vol. 210). London: UCL press.

Johnson, S., Abal, E., Ahern, K., & Hamilton, G. (2014). From science to management: using Bayesian networks to learn about Lyngbya. Statistical Science 29, 36-41.

Jolliffe, I. (2002). Principal component analysis. John Wiley & Sons, Ltd.

Karolchik, D., Barber, G., Casper, J., Clawson, H., Cline, M., Diekhans, M., Dreszer, T., Fujita, P., Guruvadoo, L., and Haeussler, M. et al. (2017). The UCSC Genome Browser database: 2014 update. Nucleic Acids Res 42, D764-D770.

Kelly, M., Alvero, A., Chen, R., Silasi, D., Abrahams, V., Chan, S., Visintin, I., Rutherford, T., and Mor, G. (2006). TLR-4 Signaling Promotes Tumor Growth and Paclitaxel Chemoresistance in Ovarian Cancer. *Cancer Research* 66, 3859-3868.

Kingma, D., & Ba, J. (2014). Adam: A method for stochastic optimization. arXiv preprint arXiv:1412.6980.

Knudson, A. G. (2001). Two genetic hits (more or less) to cancer. *Nature Reviews Cancer* 1, 157-162.

Kraan, W., Horlings, H., van Keimpema, M., Schilder-Tol, E., Oud, M., Scheepstra, C., Kluin, P., Kersten, M., Spaargaren, M., and Pals, S. (2013). High prevalence of oncogenic MYD88 and CD79B mutations in diffuse large B-cell lymphomas presenting at immune-privileged sites. *Blood Cancer Journal* 3, e139.

Lam, H., Clark, M., Chen, R., Chen, R., Natsoulis, G., O'Huallachain, M., Dewey, F., Habegger, L., Ashley, E., and Gerstein, M. et al. (2012). Performance comparison of whole-genome sequencing platforms. *Nature Biotechnology* 30, 562-562.

Lamont, R., Tan, W., Innes, A., Parboosingh, J., Schneidman-Duhovny, D., Rajkovic, A., Pappas, J., Altschwager, P., DeWard, S., and Fulton, A. et al. (2016). Expansion of phenotype and genotypic data in CRB2-related syndrome. *European Journal Of Human Genetics* 24, 1436-1444.

Landrum, M. J., Lee, J. M., Riley, G. R., Jang, W., Rubinstein, W. S., Church, D. M., & Maglott, D. R. (2014). ClinVar: public archive of relationships among sequence variation and human phenotype. *Nucleic acids research* 42, D980-D985.

LeCun, Y., Bengio, Y., & Hinton, G. (2015). Deep learning. *Nature* 521, 436-444.

Lee, E., Park, Y., & Shin, J. G. (2009). Large engineering project risk management using a Bayesian belief network. *Expert Systems with Applications* 36, 5880-5887

Lee, I., Sohn, M., Lim, H., Yoon, S., Oh, H., Shin, S., Shin, J., Oh, S., Kim, J., and Lee, D. et al. (2014). Ahnak functions as a tumor suppressor via modulation of TGF $\beta$ /Smad signaling pathway. *Oncogene* 33, 4675-4684.

Li, H., Handsaker, B., Wysoker, A., Fennell, T., Ruan, J., Homer, N., Marth, G., Abecasis, G., and Durbin, R. (2009). The Sequence Alignment/Map format and SAMtools. *Bioinformatics* 25, 2078-2079.

Linderman, M., Brandt, T., Edelmann, L., Jabado, O., Kasai, Y., Kornreich, R., Mahajan, M., Shah, H., Kasarskis, A., and Schadt, E. (2014). Analytical validation of whole exome and whole genome sequencing for clinical applications. *BMC Medical Genomics* 7.

Liu, X., Han, S., Wang, Z., Gelernter, J., & Yang, B. Z. (2013). Variant callers for next-generation sequencing data: a comparison study. *PloS one*, 8(9), e75619.

Liu, Y., Stolcke, A., Shriberg, E., & Harper, M. (2005, June). Using conditional random fields for sentence boundary detection in speech. In *Proceedings of the 43rd Annual Meeting on Association for Computational Linguistics* (pp. 451-458). Association for Computational Linguistics.

López, V., Fernández, A., García, S., Palade, V., & Herrera, F. (2013). An insight into classification with imbalanced data: Empirical results and current trends on using data intrinsic characteristics. *Information Sciences* 250, 113-141.

Lusci, A., Pollastri, G., & Baldi, P. (2013). Deep architectures and deep learning in chemoinformatics: the prediction of aqueous solubility for drug-like molecules. *Journal of chemical information and modeling* 53, 1563.

Maas, A. L., Hannun, A. Y., & Ng, A. Y. (2013, June). Rectifier nonlinearities improve neural network acoustic models. In *Proc. ICML* (Vol. 30, No. 1).

Marron, T. U., Joyce, E. Y., & Cunningham-Rundles, C. (2012). Toll-like receptor function in primary B cell defects. *Frontiers in bioscience (Elite edition)*, 4, 1853.

McKenna, A., Hanna, M., Banks, E., Sivachenko, A., Cibulskis, K., Kernytsky, A., Garimella, K., Altshuler, D., Gabriel, S., and Daly, M. et al. (2010). The Genome Analysis Toolkit: A MapReduce framework for analyzing next-generation DNA sequencing data. *Genome Research* 20, 1297-1303.

Meldrum, C., Doyle, M. A., & Tothill, R. W. (2011). Next-generation sequencing for cancer diagnostics: a practical perspective. *Clin Biochem Rev*, 32(4), 177-195.

Metzker, M. L. (2010). Sequencing technologies—the next generation. *Nature reviews genetics* 11, 31-46.

Mohiyuddin, M., Mu, J., Li, J., Bani Asadi, N., Gerstein, M., Abyzov, A., Wong, W., and Lam, H. (2015). MetaSV: an accurate and integrative structural-variant caller for next generation sequencing. *Bioinformatics* 31, 2741-2744.

Monti, S., Savage, K., Kutok, J., Feuerhake, F., Kurtin, P., Mihm, M., Wu, B., Neuberg, D., Aguiar, R., and Dal Cin, P. et al. (2005). Molecular profiling of diffuse large B-cell lymphoma identifies robust subtypes including one characterized by host inflammatory response. *Blood* 105, 1851-1861.

Moreau, Y., & Tranchevent, L. C. (2012). Computational tools for prioritizing candidate genes: boosting disease gene discovery. *Nature Reviews Genetics* 13, 523-536.

Ngo, V., Young, R., Schmitz, R., Jhavar, S., Xiao, W., Lim, K., Kohlhammer, H., Xu, W., Yang, Y., and Zhao, H. et al. (2010). Oncogenically active MYD88 mutations in human lymphoma. *Nature* 470, 115-119.

Nielsen, R., Paul, J. S., Albrechtsen, A., & Song, Y. S. (2011). Genotype and SNP calling from next-generation sequencing data. *Nature Reviews Genetics*, 12(6), 443-451.

O'Rawe, J., Jiang, T., Sun, G., Wu, Y., Wang, W., Hu, J., Bodily, P., Tian, L., Hakonarson, H., and Johnson, W. et al. (2013). Low concordance of multiple variant-calling pipelines: practical implications for exome and genome sequencing. *Genome Medicine* 5, 28.

Pearson, K. (1901). Principal components analysis. *The London, Edinburgh and Dublin Philosophical Magazine and Journal* 6, 566.

Pedregosa, F., Varoquaux, G., Gramfort, A., Michel, V., Thirion, B., Grisel, O., Blondel, M., Weiss, R., Dubourg, V., and Vanderplas, J. et al. (2017). Scikit-learn: Machine learning in Python. *Journal Of Machine Learning Research* 12, 2825-2830.

Pourret, O., Naïm, P., & Marcot, B. (Eds.). (2008). Bayesian networks: a practical guide to applications (Vol. 73). John Wiley & Sons.

Pritchard, J. K. (2001). Are rare variants responsible for susceptibility to complex diseases?. *The American Journal of Human Genetics* 69, 124-137.

Quail, M., Smith, M., Coupland, P., Otto, T., Harris, S., Connor, T., Bertoni, A., Swerdlow, H., and Gu, Y. (2012). A tale of three next generation sequencing platforms: comparison of Ion torrent, pacific biosciences and illumina MiSeq sequencers. *BMC Genomics* 13, 341.

Rehm, H. L. (2017). Evolving health care through personal genomics. *Nature Reviews Genetics*.

Ruder, S. (2016). An overview of gradient descent optimization algorithms. arXiv preprint arXiv:1609.04747.

Sandmann, S., de Graaf, A. O., Karimi, M., van der Reijden, B. A., Hellström-Lindberg, E., Jansen, J. H., & Dugas, M. (2017). Evaluating Variant Calling Tools for Non-Matched

Next-Generation Sequencing Data. *Scientific Reports* 7.

Satterwhite, E., Sonoki, T., Willis, T., Harder, L., Nowak, R., Arriola, E., Liu, H., Price, H., Gesk, S., and Steinemann, D. et al. (2001). The BCL11 gene family: involvement of BCL11A in lymphoid malignancies. *Blood* 98, 3413-3420.

Schirmer, M., D'Amore, R., Ijaz, U. Z., Hall, N., & Quince, C. (2016). Illumina error profiles: resolving fine-scale variation in metagenomic sequencing data. *BMC bioinformatics* 17, 125.

Schmidhuber, J. (2015). Deep learning in neural networks: An overview. *Neural networks* 61, 85-117.

Schork, N. J., Murray, S. S., Frazer, K. A., & Topol, E. J. (2009). Common vs. rare allele hypotheses for complex diseases. *Current opinion in genetics & development* 19, 212-219.

Shtivelman, E., Cohen, F. E., & Bishop, J. M. (1992). A human gene (AHNAK) encoding an unusually large protein with a 1.2-microns polyionic rod structure. *Proceedings of the National Academy of Sciences* 89, 5472-5476.

Silver, D., Huang, A., Maddison, C., Guez, A., Sifre, L., van den Driessche, G., Schrittwieser, J., Antonoglou, J., Panneershelvam, V., and Lanctot, M. et al. (2017). Mastering the game of Go with deep neural networks and tree search. *Nature* 529, 484-489.

Slavotinek, A. M. (2016). The Family of Crumbs Genes and Human Disease. *Molecular Syndromology* 7, 274-281.

Spencer, D., Abel, H., Lockwood, C., Payton, J., Szankasi, P., Kelley, T., Kulkarni, S., Pfeifer, J., and Duncavage, E. (2013). Detection of FLT3 Internal Tandem Duplication in Targeted, Short-Read-Length, Next-Generation Sequencing Data. *The Journal Of Molecular Diagnostics* 15, 81-93.

Schork, N. J., Murray, S. S., Frazer, K. A., & Topol, E. J. (2009). Common vs. rare allele hypotheses for complex diseases. *Current opinion in genetics & development* 19, 212-219.

Srivastava, N., Hinton, G. E., Krizhevsky, A., Sutskever, I., & Salakhutdinov, R. (2014). Dropout: a simple way to prevent neural networks from overfitting. *Journal of Machine Learning Research* 15, 1929-1958.

Su, C., Borsuk, M. E., Andrew, A., & Karagas, M. (2014, May). Incorporating prior expert knowledge in learning Bayesian networks from genetic epidemiological data. In *Computational Intelligence in Bioinformatics and Computational Biology, 2014 IEEE Conference on* (pp. 1-5). IEEE.

Suk, H. I., Lee, S. W., Shen, D., & Alzheimer's Disease Neuroimaging Initiative. (2014). Hierarchical feature representation and multimodal fusion with deep learning for AD/MCI diagnosis. *NeuroImage* 101, 569-582.

Sun, Y., Wang, X., & Tang, X. (2014). Deep learning face representation from predicting 10,000 classes. In *Proceedings of the IEEE Conference on Computer Vision and Pattern Recognition* (pp. 1891-1898).

Sutskever, I., Martens, J., Dahl, G. E., & Hinton, G. E. (2013). On the importance of initialization and momentum in deep learning. *ICML* 28, 1139-1147.

Talwalkar, A., Liptrap, J., Newcomb, J., Hartl, C., Terhorst, J., Curtis, K., Bresler, M., Song, Y., Jordan, M., and Patterson, D. (2014). SMASH: a benchmarking toolkit for human genome variant calling. *Bioinformatics* 30, 2787-2795.

Tentler, J., Tan, A., Weekes, C., Jimeno, A., Leong, S., Pitts, T., Arcaroli, J., Messersmith, W., and Eckhardt, S. (2012). Patient-derived tumour xenografts as models for oncology drug development. *Nature Reviews Clinical Oncology* 9, 338-350.

Tieleman, T. and Hinton, G. Lecture 6.5 - RMSProp, COURSERA: Neural Networks for Ma-

chine Learning. Technical report, 2012

Tsiatis, A. C., Norris-Kirby, A., Rich, R. G., Hafez, M. J., Gocke, C. D., Eshleman, J. R., & Murphy, K. M. (2010). Comparison of Sanger sequencing, pyrosequencing, and melting curve analysis for the detection of KRAS mutations: diagnostic and clinical implications. *The Journal of Molecular Diagnostics* 12, 425-432.

Uusitalo, L. (2007). Advantages and challenges of Bayesian networks in environmental modelling. *Ecological modelling*, 203(3), 312-318.

Van Der Maaten, L., Postma, E., & Van den Herik, J. (2009). Dimensionality reduction: a comparative. *J Mach Learn Res*, 10, 66-71.

Van Rossum, G. (2007, June). Python Programming Language. In USENIX Annual Technical Conference (Vol. 41, p. 36).

Wang, K., Li, M., & Hakonarson, H. (2010). ANNOVAR: functional annotation of genetic variants from high-throughput sequencing data. *Nucleic acids research* 38, e164-e164.

Wei, Z., Wang, W., Hu, P., Lyon, G. J., & Hakonarson, H. (2011). SNVer: a statistical tool for variant calling in analysis of pooled or individual next-generation sequencing data. *Nucleic acids research* 39, e132-e132.

Weniger, M., Pulford, K., Gesk, S., Ehrlich, S., Banham, A., Lyne, L., Martin-Subero, J., Siebert, R., Dyer, M., and Möller, P. et al. (2006). Gains of the proto-oncogene BCL11A and nuclear accumulation of BCL11AXL protein are frequent in primary mediastinal B-cell lymphoma. *Leukemia* 20, 1880-1882.

Windecker, S., Stortecky, S., Stefanini, G., da Costa, B., Rutjes, A., Di Nisio, M., Silletta, M., Maione, A., Alfonso, F., and Clemmensen, P. et al. (2014). Revascularisation versus medical treatment in patients with stable coronary artery disease: network meta-analysis. *BMJ* 348.

Xie, M., Lu, C., Wang, J., McLellan, M., Johnson, K., Wendl, M., McMichael, J., Schmidt, H., Yellapantula, V., and Miller, C. et al. (2014). Age-related mutations associated with clonal hematopoietic expansion and malignancies. *Nature Medicine* 20, 1472-1478.

Yan, Y., Chen, M., Shyu, M. L., & Chen, S. C. (2015, December). Deep learning for imbalanced multimedia data classification. In *Multimedia (ISM), 2015 IEEE International Symposium on* (pp. 483-488).

Ye, K., Schulz, M. H., Long, Q., Apweiler, R., & Ning, Z. (2009). Pindel: a pattern growth approach to detect break points of large deletions and medium sized insertions from paired-end short reads. *Bioinformatics* 25, 2865-2871.

Yu, L., Wang, L., & Chen, S. (2012). Exogenous or endogenous Toll-like receptor ligands: which is the MVP in tumorigenesis?. *Cellular and Molecular Life Sciences* 69, 935-949.

Zeiler, M. D. (2012). ADADELTA: an adaptive learning rate method. *arXiv preprint arXiv:1212.5701*.

Zhang, H., Gao, J., Zhao, Z., Li, M., & Liu, C. (2014). Clinical implications of SPRR1A expression in diffuse large B-cell lymphomas: a prospective, observational study. *BMC cancer* 14, 333.

Zook, J. M., Chapman, B., Wang, J., Mittelman, D., Hofmann, O., Hide, W., & Salit, M. (2014). Integrating human sequence data sets provides a resource of benchmark SNP and indel genotype calls. *Nature biotechnology* 32, 246-251.

## 7 Relevant Code

3 code segments are provided to clarify the implementation of generating the matrixes for deep learning, deep learning networks and finally bayesian networks. Other code segments not shown include the code base for parsing vcf input into features, concordance generators, NextFlow and Bash code used to simulate and process genomic data as well as to control deep learning and analytic pipelines, and other python helper scripts (e.g. comparing two VCF files, analysis with pre-trained network).

### 7.1 generate\_matrixes.py

```
1 #This python script generates the set of matrixes to be used in deep learning, and then calls the main
2   ↵ method that trains the deep learning network.
3
4 #Input : a directory that contains all the vcf files for processing, as well as a truth file.
5
6 #Output : np.arrays of features from generate_matrixes with accompanying truth labels, feature set
7   ↵ lengths, a dictionary of vcf object records, as well as the list of relevant sample features for
8   ↵ easy reference
9
10 #Notes :
11
12 #Vcf files should have the "vcf" string in their name and truth file should have a "truth" string in its
13   ↵ name.
14
15 #No other file should be present in the folder
16
17 #Overall Strategy :
18
19 #Generate a dictionary of lists, where the keys are mutations, and the value is contains a matrix
20   ↵ containing information of all five callers
21
22 #Secondly, for each mutation label, check if it is inside the truth file or not. The truth is preloaded
23   ↵ into a dictionary
24
25 #Finally, pass the set of features with accompanying truth labels to the neural network
26
27 #The main datastructure used are python dictionaries, which allows O(1) dictionary lookup times
28
29
30 import os
31 import time
32
33 from ANNgeneratorresults import * #this file contains all the main methods for actual neural network
34   ↵ training
35
36 from methods import * #this file contains all the methods for parsing each VCF entry into a numerical
37   ↵ list of features
38
39
40 #declare names of useful files that contains processed data to be saved
41 LIST_OF_INPUTS_NAME = '/ANN/samplelist.p'
42 TRUTH_DICTIONARY_NAME = '/ANN/truthdict.p'
43 CALLER_LENGTH_FILE_NAME = '/ANN/callerlengths.txt'
44 VCF_LIST_FILE_NAME = '/ANN/vcf_list.p'
45 SCORES_NAME = '/ANN/scores.txt'
46 Y_DATA_NAME = '/ANN/myydata.txt'
47 X_DATA_NAME = '/ANN/myXdata.txt'
48
49
50 #Initialise NUMBER_OF_CALLERS
```

```

28     NUMBER_OF_CALLERS = 5
29
30
31     # This method follows the typical input output processing pipeline
32     # It takes in the user input, and loads it into local variables.
33     # It then executes another method, main_analyse_samples_and_truth on the loaded variables
34     # Finally, it then saves files into a directory determined by the final variables, and calls the next
35     # step of the pipeline
36
37     def load_and_save_data(user_input):
38
39         user_input = vars(user_input)
40
41         input_samples, referencepath, output_location = load_references(user_input)    # load user input
42
43         my_x_dataset, my_y_dataset, list_of_samples, truth_dictionary, length_of_caller_outputs, \
44         vcf_record_list = main_analyse_samples_and_truth(input_samples, referencepath)
45
46         save_files(output_location, my_x_dataset, length_of_caller_outputs,
47
48             list_of_samples, truth_dictionary, vcf_record_list, my_y_dataset)
49
50         orig_stdout = sys.stdout  #save print statements into stdout
51
52         f = file(str(output_location) + SCORES_NAME, 'w')
53
54         sys.stdout = f
55
56         main_gather_input_execute_prep_output(length_of_caller_outputs, truth_dictionary, my_x_dataset,
57
58             my_y_dataset, list_of_samples, output_location, vcf_record_list)
59
60
61     # This method first prepares a dictionary of truth to be checked against. It then initialises
62     # a dictionary of samples with all the keys, each key being a variant call, and then fills it up each
63     # key with data from each caller
64
65     # subsequently, it removes dictionary entries that are the wrong size, and then checks whether
66     # each entry in the dictionary is true or not by looking up the truth dictionary
67
68     # subsequently it performs array balancing, and converts the data to np.array, as well as the dictionary
69     # of truth
70
71     # and list of called samples
72
73
74     def main_analyse_samples_and_truth(path, referencepath):
75
76         os.chdir(path)
77
78         truthdict = generate_truth_list(path)
79
80         print "truth dictionary generated at time :", time.time() - start
81
82         callerlengths, list_of_called_samples, vcf_list = generate_input(path, referencepath)
83
84         print "samples generated at time :", time.time() - start
85
86         clean_truth_array, cleaned_sample_array = check_predicted_with_truth(list_of_called_samples,
87
88             truthdict)
89
90         print "samples checked with truth at time :", time.time() - start
91
92         cleaned_sample_array = np.array(cleaned_sample_array, np.float64)
93
94         clean_truth_array = np.array(clean_truth_array)

```

```

66     return cleaned_sample_array, clean_truth_array, list_of_called_samples, truthdict, callerlengths,
67     ↵ vcf_list
68
69 # This method generates the truth dictionary, by iterating through the vcf file, parsing all the vcf
70 # entries and appending them all as keys in the dictionary
71
72 def create_truth_dictionary(generated_truth_dictionary, truth_file):
73     vcf_reader = vcf.Reader(open(truth_file, 'r'))
74     for record in vcf_reader:
75         if "GL" in record.CHROM:      #Ignore non-regular chromosomes in our dataset
76             continue
77         templist = []
78         for item in record.ALT:
79             templist.append(str(item).upper())           #Alternates might be a list, so they have to be
80             ↵ saved as a immutable tuple
81         generated_truth_dictionary[(str(record.CHROM), str(record.POS), str(record.REF).upper())] =
82             ↵ tuple(templist)
83
84 # This method generates the input dictionary, by first initialising the keys of the dictionary by
85 # iterating through the vcf file once, and then
86
87 # Iterating through the vcf file again and parsing all the entries as input vectors
88
89 def generate_input(path, referencepath):
90     reference_dictionary = get_reference_dictionary_for_entropy(referencepath)
91     base_entropy = get_ref_entropy(referencepath)
92     full_dictionary = get_dictionary_keys(path)
93     list_of_called_samples, callerlengths, vcf_list = fill_sample_dictionary(base_entropy,
94     ↵ full_dictionary, path, reference_dictionary)
95     return callerlengths, list_of_called_samples, vcf_list
96
97
98 # This method goes through all the training variant calling files and extracts unique calls as keys in
99 # the sample dictionary
100
101 def get_dictionary_keys(path):
102     sample_dictionary = {}
103     for vcf_file in os.listdir(path):
104         if ignore_file(vcf_file):
105             continue
106         vcf_reader = vcf.Reader(open(vcf_file, 'r'))
107         sample_dictionary = create_dictionary_keys(vcf_reader, sample_dictionary)
108     return sample_dictionary

```

```

102  #This method ensures the feature vector is in the right order - the entries must always be in the order
103  #→ fb, hc, ug, pindel and st.
104
105  def create_list_of_paths(path):
106
107      list_of_paths = [0] * NUMBER_OF_CALLERS
108
109      for vcf_file in os.listdir(path):
110
111          if ignore_file(vcf_file):
112
113              continue
114
115          if "fb" in vcf_file:
116
117              list_of_paths[0] = vcf_file
118
119          if "hc" in vcf_file:
120
121              list_of_paths[1] = vcf_file
122
123          if "ug" in vcf_file:
124
125              list_of_paths[2] = vcf_file
126
127          if "pind" in vcf_file:
128
129              list_of_paths[3] = vcf_file
130
131          if "st" in vcf_file:
132
133              list_of_paths[4] = vcf_file
134
135      return list_of_paths
136
137
138  # This method goes through all the training variant calling files and fills each entry in a sample
139  # dictionary
140
141  # with data. If it is empty, it returns an array of length n, where n is the number of variables
142  # that same caller would have provided.
143
144  # Each caller has a different amount of variables because it contains different datasets
145
146
147  def fill_sample_dictionary(base_entropy, sample_dictionary, path, reference_dictionary):
148
149      callerlengths = [0] * number_of_callers
150
151      index = 0
152
153      total_mode_value = 0
154
155      list_of_paths = create_list_of_paths(path)
156
157      for vcf_file in list_of_paths:
158
159          index += 1
160
161          opened_vcf_file = vcf.Reader(open(vcf_file, 'r'))
162
163          removaldict = iterate_over_file_to_extract_data(base_entropy, sample_dictionary,
164
165                                              reference_dictionary, opened_vcf_file,
166
167                                              → vcf_file)
168
169          mode_value = get_mode_value(removaldict)
170
171          add_length_to_caller_lengths_based_on_file_name(vcf_file, mode_value, callerlengths)
172
173          refill_dictionary_with_zero_arrays_for_each_file(sample_dictionary, index, mode_value)
174
175          total_mode_value += mode_value
176
177          list_of_passed_samples, vcf_list = add_mode_values_into_list_of_samples(sample_dictionary,
178
179
180                                              → total_mode_value)
181
182          return list_of_passed_samples, callerlengths, vcf_list

```

```

142
143
144 # this method fills the dictionary with empty arrays with the same length as the ones that were supposed
145 # to be added
146
147 def refill_dictionary_with_zero_arrays_for_each_file(full_dictionary, index, length_of_data_array):
148     empty_set = []
149     for i in range(length_of_data_array):
150         empty_set.append(0)
151     for item in full_dictionary:
152         checksum = len(full_dictionary[item][0])
153         if checksum < index:
154             arbinfo = empty_set
155             full_dictionary[item][0].append(arbinfo)
156
157 # this method iterates through all the files to extract data from each sample. It uses methods from the
158 # methods.py function, which parses each record for data.
159
160 def iterate_over_file_to_extract_data(base_entropy, sample_dictionary, recorddictionary, vcf_reader1,
161                                     vcf_file):
162     removaldict = {}
163     for record in vcf_reader1:
164         if "GL" in str(record.CHROM):
165             continue
166         sample_name = get_sample_name_from_record(record)
167         sample_data = getallvalues(record, recorddictionary, base_entropy, vcf_file)
168         sample_dictionary[sample_name][0].append(sample_data)
169         sample_dictionary[sample_name][1] = record
170         create_removal_dict(sample_data, removaldict)
171
172 # this method counts the mode number of entries in the dictionary. Due to certain vcf files having
173 # multiple possible number of entries for a field, this will create an error
174 # as the size of the input arrays should always be constant. Thus, any sample that does not fit the
175 # array should be removed.
176
177 def create_removal_dict(sample_data, removaldict):
178     count = 0
179     count += len(sample_data)
180     if count not in removaldict:
181         removaldict[count] = 1
182     else:

```

```

182         removaldict[count] += 1
183
184
185     # this method prepares the reference genome dictionary for use in entropy calculations
186
187     def get_reference_dictionary_for_entropy(reference_path):
188         record_dictionary = SeqIO.to_dict(SeqIO.parse(reference_path, "fasta"), key_function=get_chr)
189         return record_dictionary
190
191     # this method ensures that the files inputed are correct
192
193     def ignore_file(vcf_file):
194         if "vcf" not in vcf_file or "truth" in vcf_file:
195             return True
196         return False
197
198     # this method creates the set of keys for the dictionary
199
200     def create_dictionary_keys(vcf_reader, sample_dictionary):
201         for record in vcf_reader:
202             if "GL" in str(record.CHROM):
203                 continue
204             sample_name = get_sample_name_from_record(record)
205             sample_dictionary[sample_name] = [[], []] # fullname has become a key in fulldictionary
206         return sample_dictionary
207
208     # standard method that returns a tuple of the variant call object with the chromosome, position,
209     # reference and tuple of alternates
210
211     def get_sample_name_from_record(record):
212         templist = []
213         for item in record.ALT:
214             templist.append(str(item).upper())
215         sample_name = (str(record.CHROM), str(record.POS), str(record.REF).upper(), tuple(templist))
216         return sample_name
217
218     # this method sets the length of the input neural networks
219
220     def add_length_to_caller_lengths_based_on_file_name(vcf_file, caller_length, callerlengths):
221         if "fb" in vcf_file:
222             callerlengths[0] = caller_length
223         if "hc" in vcf_file:
224             callerlengths[1] = caller_length

```

```

225         callerlengths[2] = caller_length
226
227     if "pind" in vcf_file:
228
229         callerlengths[3] = caller_length
230
231     if "st" in vcf_file:
232
233         callerlengths[4] = caller_length
234
235
236 # this method wraps the create truth dictionary method and is used to checking that the dictionary file
237 # has the correct name
238
239
240
241 def generate_truth_list(path):
242
243     generated_truth_dictionary = {}
244
245     for truth_file in os.listdir(path):
246
247         if "truth" not in truth_file:
248
249             continue
250
251         create_truth_dictionary(generated_truth_dictionary, truth_file)
252
253     return generated_truth_dictionary
254
255
256
257 # this method takes in the mutation (in a tuple) and checks if that mutation exists in the truth
258 # dictionary
259
260 # A mutation exists if the chromosome, reference and position of the variant call is correct, AND one of
261 # the alternate alleles it contains
262
263 # is also an alternate allele in the truth dataset
264
265
266 def check_sample_against_truth_dictionary(tuple_name, final_truth_list, truth_dictionary):
267
268     temp_tuple = (tuple_name[0], tuple_name[1], tuple_name[2])
269
270     if temp_tuple in truth_dictionary:
271
272         for alternate in tuple_name[3]:
273
274             if alternate in truth_dictionary[temp_tuple]:
275
276                 final_truth_list.append(1)
277
278             return
279
280     final_truth_list.append(0)
281
282     return
283
284
285
286 # This method loads the paths of the files into local variables
287
288
289 def load_references(user_input):
290
291     file1 = user_input['input'][0]
292
293     referencepath = user_input['reference']
294
295     output_location = user_input['output']
296
297     return file1, referencepath, output_location
298
299
300
301 # This method saves all the processed data into files that can be used for other purposes later or
302 # loaded natively instead of doing the processing again
303
304

```

```

265 def save_files(output_location, x_array, length_of_caller_outputs, sample_list, truth_dict,
266     ↵ vcf_dictionary_file,
267         y_array=[]):
268
269     file2 = output_location
270
271     x_data_file_name = str(file2) + str(X_DATA_NAME)
272
273     np.save(x_data_file_name, x_array)
274
275     vcf_file_name = str(file2) + str(VCF_LIST_FILE_NAME)
276
277     caller_length_file_name = str(file2) + str(CALLER_LENGTH_FILE_NAME)
278
279     truth_dictionary_name = str(file2) + str(TRUTH_DICTIONARY_NAME)
280
281     list_of_inputs_name = str(file2) + str(LIST_OF_INPUTS_NAME)
282
283     np.save(caller_length_file_name, length_of_caller_outputs)
284
285     with open(list_of_inputs_name, 'wb') as samplesave1:
286
287         pickle.dump(sample_list, samplesave1)
288
289     with open(truth_dictionary_name, 'wb') as samplesave2:
290
291         pickle.dump(truth_dict, samplesave2)
292
293     with open(vcf_file_name, 'wb') as samplesave3:
294
295         pickle.dump(vcf_dictionary_file, samplesave3)
296
297     if y_array != []:
298
299         y_data_file_name = str(file2) + str(Y_DATA_NAME)
300
301         np.save(y_data_file_name, y_array)
302
303
304     # This method takes in two dictionaries, a dictionary of truth mutations and a dictionary of sample
305     ↵ mutations,
306
307     # checks whether each of the sample variables are inside the truth dictionary
308
309     # and returns 2 arrays, an array of samples and an array of accompanying truth labels
310
311
312     def check_predicted_with_truth(passed_list_of_samples, dictionary_of_truth=[]):
313
314         final_array_of_samples = []
315
316         final_truth_list = []
317
318         for item in passed_list_of_samples:
319
320             if dictionary_of_truth:
321
322                 check_sample_against_truth_dictionary(item[0], final_truth_list, dictionary_of_truth)
323
324                 temp_array = []
325
326                 for row in item[1]:
327
328                     temp_array.extend(row)
329
330                 final_array_of_samples.append(temp_array)
331
332             if dictionary_of_truth:
333
334                 return final_truth_list, final_array_of_samples
335
336         return final_array_of_samples
337
338
339     # This method ensures that only the variables that have the modal number of features are used
340
341     # in neural network training to ensure all array sizes are the same
342
343
344     def add_mode_values_into_list_of_samples(full_dictionary, mode_value):

```

```

307     list_of_passed_samples = []
308     vcf_list = []
309     for key in full_dictionary:
310         second_count = 0
311         for item in full_dictionary[key][0]:
312             second_count += len(item)
313         if second_count != mode_value:
314             continue
315         list_of_passed_samples.append([key, full_dictionary[key][0]])
316         vcf_list.append(full_dictionary[key][1])
317     return list_of_passed_samples, vcf_list
318
319 # This method gets the modal number of features from a modal dictionary
320
321 def get_mode_value(removaldict):
322     curr = 0
323     mode_value = 0
324     for new_key in removaldict:
325         if removaldict[new_key] > curr:
326             curr = removaldict[new_key]
327             mode_value = new_key
328     return mode_value
329
330 # This method iterates through the dataset to create a modal dictionary which contains a key-value pair
331 # ← of (number of features - number of times seen).
332 # The mode number of features is kept
333
334 def iterate_through_dictionary_to_find_mode_size(full_dictionary):
335     removaldict = {}
336     samples = 0
337     for key in full_dictionary:
338         samples += 1
339         if samples == sample_limit:
340             break
341         count = 0
342         for item in full_dictionary[key]:
343             count += len(item)
344         if count not in removaldict:
345             removaldict[count] = 1
346         else:
347             removaldict[count] += 1
348     return removaldict
349

```

```
350 if __name__ == "__main__":
351     np.seterr(divide='raise', invalid='raise')
352
353     parser = argparse.ArgumentParser(description="train neural net")
354
355     parser.add_argument('-i', '--input', help="give directories with files", nargs='+')
356     parser.add_argument('-d', '--debug', help="look at matrixes built")
357     parser.add_argument('-r', '--reference', help="")
358     parser.add_argument('-o', '--output', help="")
359
360     paths = parser.parse_args()
361
362     start = time.time()
363
364     load_and_save_data(paths)
```

## 7.2 train\_network.py

```
1 #This script is called by the generate_matrixes.py script and contains the implementation of the neural
2 → network.
3
4 #Input : np.array of features from generate_matrixes with accompanying truth labels, feature set
5 → lengths, a dictionary of vcf object records, as well as the list of sample features
6
7 #Output : A VCF file containing all the filtered entries by the neural network, as well the list of
8 → accompanying scores
9
10 #Overall Strategy :
11
12 #Perform SMOTE oversampling of the input features, and then use the features to train the neural network
13
14 #After training, perform validation on test dataset, and subsequently prepare a vcf file with filtered
15 → entries
16
17
18
19
20
21
22
23
24
25
26
27 #set constants
```

```

28     PCA_COMPONENTS = 8
29     STEP_INCREMENT = 10
30     RECURSION_LIMIT = 0.0002
31     VERBOSE = 1
32     seed = 1337
33
34     # Initialise random seed for reproducibility
35     np.random.seed(seed)
36
37     #Prepare file names for saving
38     vcf_file_name = "/ANN/truevcf.vcf"
39     keras_model_name = "/ANN/model"
40     model_truth_name = "/ANN/modeltruths.txt"
41     model_predictions_name = "/ANN/modelpredictions.txt"
42     original_vcf_reader = "/data/backup/metacaller/stage/data/version6.3a/hc.vcf.normalisedtrain.vcf"
43
44     # this method takes in a path and returns training matrixes for the ANN
45     # The path should contain n caller vcf files and 1 truth file
46     # vcf files should be labelled with vcf and truth file should be labelled with truth
47     # no other file should be present in the folder
48     def main_gather_input_execute_prep_output(array_sizes, dict_of_truth_input, fullmatrix_sample,
49         ↪ fullmatrix_truth, list_of_samples_input, save_location, vcf_dictionary):
50         calculated_prediction_actual, calculated_truth_actual = train_neural_net(20, 10, fullmatrix_sample,
51             ↪ fullmatrix_truth,
52             ↪ save_location, array_sizes)
53         get_all_relevant_scores(calculated_prediction_actual, calculated_truth_actual, dict_of_truth_input,
54             ↪ list_of_samples_input, vcf_dictionary, save_location)
55
56     # This method counts the number of false negatives inside the input sample
57
58     def count_false_negative(calculated_prediction_actual, calculated_truth_actual):
59         count_false_negative = 0
60         for i in range(len(calculated_prediction_actual)):
61             if calculated_prediction_actual[i] == 0 and calculated_truth_actual[i] == 1:
62                 count_false_negative += 1
63         return count_false_negative
64
65     # this is the wrapper function for the recursive hill climbing algorithm to get the best f1 score
66     # It starts from a low threshold value, and marginally increases the threshold until it is unable to
67     ↪ find
68     # any better F1 scores. It then reports the threshold, F1 score and produces the filtered callset
69
70     def get_all_relevant_scores(calculated_prediction_actual, calculated_truth_actual, dict_of_truth_input,
71         list_of_samples_input, vcf_list, outputpath):

```

```

67     print "Here are some predictions", calculated_prediction_actual[:100]
68     print "here are some truths", calculated_prediction_actual[:100]
69     f1_score_left = get_scores(calculated_prediction_actual, calculated_truth_actual, 0.0,
70         ↪ list_of_samples_input, dict_of_truth_input)
71     guess_f1_final_score, guess_f1_final = recursive_best_f1_score(calculated_prediction_actual,
72         ↪ calculated_truth_actual, dict_of_truth_input, list_of_samples_input, 0.0, f1_score_left, 0.2)
73     get_scores(calculated_prediction_actual, calculated_truth_actual, guess_f1_final,
74         ↪ list_of_samples_input, dict_of_truth_input, VERBOSE)
75     produce_vcf_file(calculated_prediction_actual, guess_f1_final, list_of_samples_input, vcf_list,
76         ↪ outputpath)

77
78 # This method produces the vcf file through filtering with the neural network threshold calls
79
80
81 def produce_vcf_file(calculated_prediction_actual, guess_f1_final, list_of_samples_input, vcf_list,
82     ↪ outputpath):
83     prediction = []
84     for item in calculated_prediction_actual:
85         if item > guess_f1_final:
86             prediction.append(1)
87         else:
88             prediction.append(0)
89     list_of_records = []
90     for i in range(len(list_of_samples_input)):
91         if prediction[i] == 1:
92             list_of_records.append(vcf_list[i])
93     vcf_reader = vcf.Reader(filename=original_vcf_reader)
94     vcf_writer = vcf.Writer(open(outputpath + vcf_file_name, 'w'), vcf_reader)
95     for record in list_of_records:
96         vcf_writer.write_record(record)

97
98 # This method is the recursive function that attempts to find the threshold that produces the best f1
99 # score. It does this
100 # by iterating through steps of thresholds (0.2, 0.02 and 0.002) until no better F1 score can be found
101 # for a marginal increase in threshold.
102 # It then returns the best F1 score and the threshold
103
104 def recursive_best_f1_score(calculated_prediction_actual, calculated_truth_actual, dict_of_truth_input,
105     list_of_samples_input, guess, guess_score, step):
106     if step <= RECURSION_LIMIT:
107         return guess_score, guess
108     new_guess = guess + step
109     new_guess_score = get_scores(calculated_prediction_actual, calculated_truth_actual, new_guess,
110         list_of_samples_input, dict_of_truth_input)
111     if new_guess_score > guess_score:

```

```

104     return recursive_best_f1_score(calculated_prediction_actual, calculated_truth_actual,
105                                     ↪ dict_of_truth_input,
106                                     list_of_samples_input, new_guess, new_guess_score, step)
107
108     return recursive_best_f1_score(calculated_prediction_actual, calculated_truth_actual,
109                                     ↪ dict_of_truth_input,
110                                     list_of_samples_input, guess, guess_score, step / STEP_INCREMENT)
111
112
113 # this method uses pre-loaded data to train the neural network. It is optional and only used when this
114 # python script is called natively and not imported
115
116 def load_references(input_paths):
117
118     input_paths = vars(input_paths)
119
120     fullmatrix_sample = np.load(input_paths['input'][0])
121
122     fullmatrix_truth = np.load(input_paths['input'][1])
123
124     with open(input_paths['input'][3], 'rb') as fp1:
125
126         list_of_samples_input = pickle.load(fp1)
127
128     with open(input_paths['input'][4], 'rb') as fp2:
129
130         dict_of_truth_input = pickle.load(fp2)
131
132     array_sizes = np.load(input_paths['input'][5])
133
134     with open(input_paths['input'][6], 'rb') as fp3:
135
136         vcf_dictionary = pickle.load(fp3)
137
138     orig_stdout = sys.stdout
139
140     f = file(str(input_paths['input'][3]) + '.txt', 'w')
141
142     sys.stdout = f
143
144     return array_sizes, dict_of_truth_input, fullmatrix_sample, fullmatrix_truth,
145     ↪ list_of_samples_input, input_paths, vcf_dictionary
146
147 # this method solves the double false negative problem that is created due to the neural network
148 # prediction scheme
149
150
151 def remove_duplicated_false_negative(prediction_list, truth_list, false_negatives):
152
153     count = 0
154
155     removal_list = []
156
157     for i in range(len(prediction_list) - 1, -1, -1):
158
159         if count == false_negatives:
160
161             break
162
163         if prediction_list[i] == 0 and truth_list[i] == 1:
164
165             removal_list.insert(0, i)
166
167             count += 1
168
169         for index in removal_list:
170
171             prediction_list.pop(index)
172
173             truth_list.pop(index)
174
175     return prediction_list, truth_list

```

```

143 # this method takes in the binary truth and predicted samples and calculates the true positive rate,
144 # false positive rate, recall, precision and f1 score
145
146 def get_scores(actual_predictions, actual_truth, value, sample_list, truth_dictionary, verbose=0):
147     temp_actual_truth = list(actual_truth)
148     prediction = []
149     for item in actual_predictions:
150         if item > value:
151             prediction.append(1)
152         else:
153             prediction.append(0)
154     false_negatives = count_false_negative(actual_predictions, actual_truth)
155     finalpredictionnumbers, finaltruthnumbers = add_negative_data(sample_list, truth_dictionary,
156     ↪ prediction, temp_actual_truth)
157     finalpredictionnumbers, finaltruthnumbers =
158     ↪ remove_duplicated_false_negative(finalpredictionnumbers, finaltruthnumbers, false_negatives)
159     final_f1_score = f1_score(finaltruthnumbers, finalpredictionnumbers)
160     if verbose:
161         print_scores(actual_truth, final_f1_score, finalpredictionnumbers, finaltruthnumbers,
162         ↪ prediction, value)
163     return final_f1_score
164
165
166 # default method for printing all relevant scores
167
168 def print_scores(actual_truth, final_f1_score, finalpredictionnumbers, finaltruthnumbers, prediction,
169     ↪ value):
170     final_false_positive, final_true_negative = perf_measure(finaltruthnumbers, finalpredictionnumbers)
171     print "final false positive rate is :", final_false_positive
172     print "final true negative rate is :", final_true_negative
173     print "final precision score is :", precision_score(finaltruthnumbers, finalpredictionnumbers)
174     print "final recall score is :", recall_score(finaltruthnumbers, finalpredictionnumbers)
175     print "threshold is", value
176     print "final F1 score is : ", final_f1_score
177
178 # This method looks at the set of predicted samples and the set of truths and adds the false negatives
179 # to the predicted sample.
180
181 def add_negative_data(list_of_samples, dict_of_truth, array_of_predicted, array_of_truth):
182     dict_of_samples = generate_sample_dictionary(array_of_predicted, list_of_samples)
183     list_of_truth = generate_list_of_truth(dict_of_truth)
184     new_array_of_predicted = list(array_of_predicted)
185     new_array_of_truth = list(array_of_truth)
186     original_length = len(new_array_of_predicted)
187     for item in list_of_truth:

```

```

181     fillnegative(item, dict_of_samples, new_array_of_predicted, new_array_of_truth)
182     print "number of false data samples are", (len(new_array_of_predicted) - original_length)
183     return new_array_of_predicted, new_array_of_truth
184
185 # This method generates a list of truth variant calls from a dictionary of truth variant calls.
186
187 def generate_list_of_truth(dict_of_truth):
188     list_of_truth = []
189     for key in dict_of_truth:
190         mytuple = dict_of_truth[key]
191         temptuple = []
192         for item in mytuple:
193             temptuple.append(item)
194         list_of_truth.append([key[0], key[1], key[2], temptuple])
195     return list_of_truth
196
197 # This method generates a dictionary of sample variant calls from a list of sample variant calls.
198
199 def generate_sample_dictionary(array_of_predicted, list_of_samples):
200     dict_of_samples = {}
201     for i in range(len(list_of_samples)):
202         item = list_of_samples[i]
203         if array_of_predicted[i] == 0:
204             continue
205         new_key = (item[0][0], item[0][1], item[0][2])
206         new_value = item[0][3]
207         if new_key not in dict_of_samples:
208             dict_of_samples[new_key] = new_value
209         else:
210             dict_of_samples[new_key] = list(dict_of_samples[new_key])
211             dict_of_samples[new_key].extend(new_value)
212             dict_of_samples[new_key] = tuple(dict_of_samples[new_key])
213             # print dict_of_samples[new_key]
214     return dict_of_samples
215
216 # Actual method to calculate false positive, false negative rates
217
218 def perf_measure(y_actual, y_hat):
219     true_positive = 0
220     false_positive = 0
221     false_negative = 0
222     true_negative = 0
223
224     for i in range(len(y_hat)):
```

```

225     if y_actual[i] == 1 and y_hat[i] == 1:
226         true_positive += 1
227     for i in range(len(y_hat)):
228         if y_hat[i] == 1 and y_actual[i] == 0:
229             false_positive += 1
230     for i in range(len(y_hat)):
231         if y_actual[i] == 1 and y_hat[i] == 0:
232             false_negative += 1
233     for i in range(len(y_hat)):
234         if y_hat[i] == 0 and y_actual[i] == 0:
235             true_negative += 1
236
237     print "true positives :", true_positive
238     print "false positives :", false_positive
239     print "false negatives :", false_negative
240     print "true negatives :", true_negative
241
242     true_positive = float(true_positive)
243     false_positive = float(false_positive)
244     false_negative = float(false_negative)
245     if false_positive == 0 and true_positive == 0:
246         false_positive_rate = 0
247     else:
248         false_positive_rate = false_positive / (false_positive + true_positive)
249     if false_negative == 0 and true_positive == 0:
250         true_negative_rate = 0
251     else:
252         true_negative_rate = false_negative / (false_negative + true_positive)
253
254     return false_positive_rate, true_negative_rate
255
256
257 # comparator method that takes a tuple and checks whether it is in the dictionary of samples, if it is
258 # not, then add a false negative call to the dataset
259
260 def fillnegative(tuple1, sampledict, arrayofsamples, arrayoftruths):
261     tuple2 = (tuple1[0], tuple1[1], tuple1[2])
262     if tuple2 in sampledict:
263         for ALT in tuple1[3]:
264             if ALT in sampledict[tuple2]:
265                 return
266             arrayofsamples.append(0)
267             arrayoftruths.append(1)
268

```

```

268 # main method that performs neural network training. This method takes in the sample matrixes, the truth
269 # variables, a save file location, number of epochs,
270 # size of input arrays and the minibatch training size. It first performs SMOTE on the input dataset,
271 # then splits it into training and test dataset. It then
272 # initialises the deep learning layers, compiles the neural network and uses the input data to fit the
273 # network. The best set of weights at any point is saved
274 # to a file and reloaded at the end of the fitting. After training, the neural network is used to
275 # predict the original un-oversampled dataset
276
277 def train_neural_net(mybatch_size, mynb_epoch, myX_train, myy_train, location, arraysize):
278     fb_size, hc_size, ug_size, pindel_size, st_size = get_sizes(array_sizes)
279     X_resampled, y_resampled = do_smote_resampling(myX_train, myy_train)
280     X_train, X_test, y_train, y_test = train_test_split(X_resampled, y_resampled,
281                                                       test_size=0.33, random_state=seed)
282     X_fb, X_hc, X_ug, X_pindel, X_st = prep_input_samples(array_sizes, X_train)
283     X_fb_test, X_hc_test, X_ug_test, X_pindel_test, X_st_test = prep_input_samples(array_sizes, X_test)
284     batch_size = mybatch_size
285     nb_epoch = mynb_epoch
286
287     fb_branch = Sequential()
288     develop_first_layer_matrixes(fb_branch, fb_size)
289
290     hc_branch = Sequential()
291     develop_first_layer_matrixes(hc_branch, hc_size)
292
293     ug_branch = Sequential()
294     develop_first_layer_matrixes(ug_branch, ug_size)
295
296     pindel_branch = Sequential()
297     develop_first_layer_matrixes(pindel_branch, pindel_size)
298
299     st_branch = Sequential()
300     develop_first_layer_matrixes(st_branch, st_size)
301
302     final_model = Sequential()
303     final_model.add(Merge([fb_branch, hc_branch, ug_branch, pindel_branch, st_branch], mode='concat',
304                           concat_axis=1))
305     final_model.add(Dense(24, activation='linear'))
306     final_model.add(LeakyReLU(alpha=0.05))
307     final_model.add(Dense(6, activation='linear'))
308     final_model.add(LeakyReLU(alpha=0.05))
309     final_model.add(Dense(1, activation='linear'))
310     final_model.add(Activation('sigmoid'))
311     print (final_model.summary())

```

```

307     adam = Adam(lr=0.00001, rho=0.9, epsilon=1e-08, decay=0.0)
308     final_model.compile(loss='binary_crossentropy',
309                           optimizer=adam,
310                           metrics=['accuracy'])
311
312     filepath = location + "/best_weights.hdf5"
313     checkpoint = ModelCheckpoint(filepath, monitor='val_acc', verbose=1, save_best_only=True,
314                                  mode='max')
315     callbacks_list = [checkpoint]
316     model_history = final_model.fit([X_train], y_train, batch_size=batch_size, nb_epoch=nb_epoch,
317                                     validation_split=0.2, verbose=2, callbacks=callbacks_list)
317     final_model = load_model(location + "/best_weights.hdf5")
318     print model_history.history['val_acc'], model_history.history['val_acc']
319     print model_history.history['val_loss'], model_history.history['val_loss']
320     np.save(location + "/best_weights.hdf5", model_history.history['val_acc'])
321     np.save(location + "/best_weights.hdf5", model_history.history['val_loss'])
322     scores = final_model.evaluate([X_test], y_test)
323     print scores
324     final_prediction_array_probabilities = final_model.predict([myX_train])
325     final_prediction_array_probabilities = np.squeeze(final_prediction_array_probabilities)
326     save_model_details(final_model, final_prediction_array_probabilities, myy_train, location)
327
328     return final_prediction_array_probabilities, myy_train
329
330 # method to build 8 layer neural network stack
331
332 def develop_first_layer_matrixes(neural_net_branch, branch_size):
333     neural_net_branch.add(BatchNormalization(input_shape=(branch_size,), axis=1))
334     neural_net_branch.add(Dense(24, activation='linear'))
335     neural_net_branch.add(LeakyReLU(alpha=0.05))
336     neural_net_branch.add(Dense(24, activation='linear'))
337     neural_net_branch.add(LeakyReLU(alpha=0.05))
338     neural_net_branch.add(Dense(24, activation='linear'))
339     neural_net_branch.add(LeakyReLU(alpha=0.05))
340     neural_net_branch.add(Dense(24, activation='linear'))
341     neural_net_branch.add(LeakyReLU(alpha=0.05))
342     neural_net_branch.add(Dense(24, activation='linear'))
343     neural_net_branch.add(LeakyReLU(alpha=0.05))
344     neural_net_branch.add(Dense(24, activation='linear'))
345     neural_net_branch.add(LeakyReLU(alpha=0.05))
346     neural_net_branch.add(Dropout(0.2))
347     neural_net_branch.add(Dense(24, activation='linear'))
348     neural_net_branch.add(LeakyReLU(alpha=0.05))
349     neural_net_branch.add(Dropout(0.2))

```

```

350     neural_net_branch.add(Dense(6, activation='linear'))
351     neural_net_branch.add(LeakyReLU(alpha=0.05))
352
353     # Method to perform SMOTE oversampling
354
355     def do_smote_resampling(myX_train, myy_train):
356         sm = SMOTE(kind='regular')
357         where_are_NaNs = np.isnan(myX_train)
358         myX_train[where_are_NaNs] = 0
359         X_resampled, y_resampled = sm.fit_sample(myX_train, myy_train)
360
361         return X_resampled, y_resampled
362
363
364     # this method saves the details of the neural network
365
366
367     def save_model_details(final_model, save_model_probabilities, truthtable, location):
368
369         name1 = location + model_predictions_name
370         name2 = location + model_truth_name
371         name3 = location + keras_model_name
372
373         np.save(name1, save_model_probabilities)
374         np.save(name2, truthtable)
375         final_model.save(name3)
376
377
378     # this method gets the array size of the features used
379
380
381     def get_sizes(array_sizes):
382
383         fb_size = array_sizes[0]
384         hc_size = array_sizes[1]
385         ug_size = array_sizes[2]
386         pindel_size = array_sizes[3]
387         st_size = array_sizes[4]
388
389         return fb_size + hc_size + ug_size + pindel_size + st_size
390
391
392
393     # this method uses a map function to filter data such that each merge layer gets the correct set of data
394
395     def prep_input_samples(array_sizes, x_training_data):
396
397         count = 0
398
399         X_fb = np.array(map(lambda x: x[count:array_sizes[0]], x_training_data))
400         count += array_sizes[0]
401
402         X_hc = np.array(map(lambda x: x[count:count + array_sizes[1]], x_training_data))
403         count += array_sizes[1]
404
405         X_ug = np.array(map(lambda x: x[count:count + array_sizes[2]], x_training_data))
406         count += array_sizes[2]
407
408         X_pindel = np.array(map(lambda x: x[count:count + array_sizes[3]], x_training_data))

```

```
394     count += array_sizes[3]
395
396     X_st = np.array(map(lambda x: x[count:count + array_sizes[4]], x_training_data))
397     count += array_sizes[4]
398
399     return X_fb, X_hc, X_ug, X_pindel, X_st
400
401 if __name__ == "__main__":
402
403     parser = argparse.ArgumentParser(description="train neural net")
404
405     parser.add_argument('-i', '--input', help="give directories with files", nargs='+')
406
407     input_path = parser.parse_args()
408
409     array_sizes, dict_of_truth_input, fullmatrix_sample, fullmatrix_truth, \
410     list_of_samples_input, paths, vcf_dictionary = load_references(input_path)
411
412     main_gather_input_execute_prep_output(array_sizes, dict_of_truth_input, fullmatrix_sample,
413                                         ↴ fullmatrix_truth, list_of_samples_input, paths, vcf_dictionary)
```

## 7.3 compute\_bayesian.py

```
1 #This script takes in a VCF file with functional annotation already done, and computes the bayesian
2   ↳ network using the annotations. It produces a sorted list of vcf entries in a text file, with
3   ↳ accompanying annotation scores
4
5 #Input : VCF file with functional annotation
6
7 #Output : A sorted list of vcf entries with accompanying annotation scores, redirected from stdout to a
8   ↳ file
9
10 #Overall Strategy :
11
12 #First extract all the features from the vcf files and then perform feature-wise normalisation.
13
14 #Subsequently, prepare the bayesian network by creating edges, nodes, preparing prior distributions
15
16 #Finally use features to update the bayesian network to obtain final probabilities for importance
17
18 #Report a list of sorted probabilitites for easy ranking
19
20
21
22
23
24
25
```

```

26     # sys.stdout = f
27     return opened_vcf_file
28
29 #method for getting functional annotation scores
30
31 def get_scores(record):
32     list_of_important_mutations = [record.INFO['SIFT_score'], record.INFO['LRT_score'],
33                                     record.INFO['MutationAssessor_score'],
34                                     record.INFO['Polyphen2_HVAR_score'], record.INFO['FATHMM_score']]
35
36     if 'NN_prediction' in record.INFO:
37         NN_prediction = record.INFO['NN_prediction'][0]
38     else:
39         NN_prediction = -1
40
41     list_of_important_mutations = map(lambda x: x[0], list_of_important_mutations)
42     list_of_important_mutations = map(lambda x: None if x == None else float(x),
43                                      list_of_important_mutations)
44
45     return NN_prediction, list_of_important_mutations
46
47 #main method that controls I/O - it gets the input, applies the main function and then prepares the
48 #                                output
49
50 def main(paths):
51     vcf_object = load_reference(paths)
52     full_list_of_scores = analyse_main(vcf_object)
53     prepare_output(full_list_of_scores)
54
55 #this method controls the processes applied to the vcf file - for each record, it extract the list of
56 #                                scores,
57 # normalises it, compute probabilities, sorts it and then return output
58
59 def analyse_main(vcf_object):
60     full_list_of_scores = extract_list_of_scores(vcf_object)
61     apply_feature_wise_normalisation(full_list_of_scores)
62     compute_network_and_probabilities(full_list_of_scores)
63     full_list_of_scores.sort(key=lambda x: x[4], reverse=True)
64
65     return full_list_of_scores
66
67 # since print is redirected to stdoutput, print function is used to store output
68
69 def prepare_output(full_list_of_scores):
70     for item in full_list_of_scores:
71         print item[2], item, item[2].INFO['Gene.refGene']
72
73 # wrapper function used to create bayesian network for all records

```

```

67
68 def compute_network_and_probabilities(full_list_of_scores):
69     for record in full_list_of_scores:
70         network = create_network_and_compute_probabilities(record)
71         compute_record(network, record)
72
73     # this function applies a featurewise normalisation of all features to a range of 0-1, and flip scores
74     # for certain features
75
76 def apply_feature_wise_normalisation(full_list_of_scores):
77     for i in range(6):
78         min_num = 1000000
79         max_num = -1000000
80         for item in full_list_of_scores:
81             if item[1][i] != None:
82                 min_num = min(min_num, item[1][i])
83                 max_num = max(max_num, item[1][i])
84         for item in full_list_of_scores:
85             if item[1][i] != None:
86                 value = ((item[1][i] - min_num) / (max_num - min_num) + 0.2) / 1.3
87                 item[1][i] = value
88             else:
89                 item[1][i] = 0.5
90         if i == 0 or i == 5:
91             for item in full_list_of_scores:
92                 if item[1][i] != None:
93                     item[1][i] = -item[1][i]
94
95     # extract list of of scores from each record, including all functional annotations, clinvar scores and
96     ↵ dbsnp
97
98 def extract_list_of_scores(vcf_object):
99     count = 0
100    full_list_of_scores = []
101    for record in vcf_object:
102        count += 1
103        nn_prediction, list_of_scores = get_scores(record)
104        if not list(filter(lambda x: x != None, list_of_scores)):
105            continue
106        get_clinvar_scores(list_of_scores, record)
107        snp_present = get_db_snp_scores(record)
108        full_list_of_scores.append([float(nn_prediction), list_of_scores, record, snp_present])
109
110    return full_list_of_scores

```

```

110  # Compute the Bayesian Network by assuming observations and attaching mapped probabilities (0,1) to
111    ↳ P(X=True / Y=True)

112  def compute_record(network, record):
113      beliefs = network.predict_proba({'Real Gene': 'True', 'ClinVar': 'True', 'PolyPhen': 'True', 'LRT':
114          ↳ 'True', 'MutationAssessor': 'True', 'SIFT': 'True', 'FATHMM_gene': 'True', 'rs_gene': 'True'})
115      # print "\n".join("{}\t{}".format(state.name, belief) for state, belief in zip(network.states,
116          ↳ beliefs))
117      # get the probability that the gene is important
118      prob_gene_important = beliefs[2].values()[1]
119      beliefs = map(str, beliefs)
120      record.append(prob_gene_important)
121      record.append(record[2].INFO['snp138'])
122      record.append(record[3])
123
124      # If snp is present in db-snp, attach probability of importance to 0.3, else 0.7
125
126      def get_db_snp_scores(record):
127          snp_present = 0.7
128          if record.INFO['snp138'][0] != None:
129              snp_present = 0.3
130          return snp_present
131
132      # If snp is present in clinvar, attach probability of importance to 0.7, else 0.3
133
134      def get_clinvar_scores(list_of_scores, record):
135          if record.INFO['clinvar_20150629'][0] != None:
136              list_of_scores.append(0.7)
137          else:
138              list_of_scores.append(0.3)
139
140      # wrapper method to create the bayesian network and compute probabilities
141
142      def create_network_and_compute_probabilities(record):
143          ClinVar_gene, FATHMM_gene, LRT_gene, MutationAssessor_gene, MutationTaster_gene, PolyPhen2_gene,
144          ↳ SIFT_gene, functional_gene, importgene, real_gene, rs_gene = initialise_distributions(
145          record)
146          # set up states
147          s1, s10, s11, s2, s3, s4, s5, s6, s7, s8, s9 = generate_states(ClinVar_gene, FATHMM_gene, LRT_gene,
148          ↳ MutationAssessor_gene, MutationTaster_gene, PolyPhen2_gene, SIFT_gene, functional_gene,
149          ↳ importgene, real_gene, rs_gene)
150          # set up network
151          network = add_edges_bake_network(s1, s10, s11, s2, s3, s4, s5, s6, s7, s8, s9)
152          return network

```

```

148
149 # method to create the edges in the network
150
151 def add_edges_bake_network(s1, s10, s11, s2, s3, s4, s5, s6, s7, s8, s9):
152     network = BayesianNetwork("Gene Prediction")
153     network.add_states(s1, s2, s3, s4, s5, s6, s8, s9, s10, s11)
154     network.add_edge(s1, s3)
155     network.add_edge(s2, s3)
156     network.add_edge(s4, s2)
157     network.add_edge(s5, s2)
158     network.add_edge(s6, s2)
159     network.add_edge(s7, s2)
160     network.add_edge(s8, s2)
161     network.add_edge(s9, s2)
162     network.add_edge(s10, s2)
163     network.add_edge(s11, s3)
164     network.bake()
165     return network
166
167 # method that generates the nodes in the bayesian network
168
169 def generate_states(ClinVar_gene, FATHMM_gene, LRT_gene, MutationAssessor_gene, MutationTaster_gene,
170                     PolyPhen2_gene, SIFT_gene, functional_gene, importgene, real_gene, rs_gene):
171     s1 = State(real_gene, name="Real Gene")
172     s2 = State(functional_gene, name="Functional Gene")
173     s3 = State(importgene, name="Important Gene")
174     s4 = State(ClinVar_gene, name="ClinVar")
175     s5 = State(PolyPhen2_gene, name="PolyPhen")
176     s6 = State(LRT_gene, name="LRT")
177     s7 = State(MutationTaster_gene, name="MutationTaster")
178     s8 = State(MutationAssessor_gene, name="MutationAssessor")
179     s9 = State(SIFT_gene, name="SIFT")
180     s10 = State(FATHMM_gene, name="FATHMM_gene")
181     s11 = State(rs_gene, name="rs_gene")
182
183 #methods to initialise prior distributions in bayesian network
184
185 def initialise_distributions(record):
186     ClinVar_gene = DiscreteDistribution({'True': 0.5, 'False': 0.5})
187     PolyPhen2_gene = DiscreteDistribution({'True': 0.5, 'False': 0.5})
188     LRT_gene = DiscreteDistribution({'True': 0.5, 'False': 0.5})
189     MutationTaster_gene = DiscreteDistribution({'True': 0.5, 'False': 0.5})
190     MutationAssessor_gene = DiscreteDistribution({'True': 0.5, 'False': 0.5})

```

```

191     SIFT_gene = DiscreteDistribution({'True': 0.5, 'False': 0.5})
192     FATHMM_gene = DiscreteDistribution({'True': 0.5, 'False': 0.5})
193     rs_gene = DiscreteDistribution({'True': 0.5, 'False': 0.5})
194     import_cdp = get_cdp(3, [(record[0] + 0.2) / 1.3, record[3], 0.8])
195     functional_cdp = get_cdp(6, record[1])
196     functional_gene = ConditionalProbabilityTable(functional_cdp, [ClinVar_gene, PolyPhen2_gene,
197                                                 ↪ LRT_gene,
198                                                 MutationAssessor_gene,
199                                                 SIFT_gene, FATHMM_gene])
200     real_gene = DiscreteDistribution({'True': 0.5, 'False': 0.5})
201     importgene = ConditionalProbabilityTable(import_cdp, [real_gene, rs_gene, functional_gene])
202     return ClinVar_gene, FATHMM_gene, LRT_gene, MutationAssessor_gene, MutationTaster_gene,
203             ↪ PolyPhen2_gene, SIFT_gene, functional_gene, importgene, real_gene, rs_gene
204
205
206
207     # method that builds the cdp table. n is the number of input variables, probability list gives the
208     ↪ probability
209     # that the i-th X variable is true P(Xi=True).
210
211
212
213     # Generates a True False matrix using binary counting logic, critical for input in bayesian network
214
215     def create_true_false_matrix(n):
216         temp_list = []
217         calculate_probabilities(n, prob_list, temp_list)
218         return temp_list
219
220
221
222     # Generates a True False matrix using binary counting logic, critical for input in bayesian network
223
224     def get_cdp(n, prob_list):
225         temp_list = create_true_false_matrix(n)
226         calculate_probabilities(n, prob_list, temp_list)
227         return temp_list
228
229
230

```

```

231  # calculates the probabilities, taking in the true list as well as a list of probabilities. The key here
232  ↪   is
233  # the probability that the mutation is true is related to the scores given by mutation taster etc..
234  # ie  $P(X \text{ is impt} | X \text{ is Clinvar}) = P(X \text{ is Clinvar})$ 
235
236  def calculate_probabilities(n, prob_list, temp_list):
237      for i in range(0, 2 ** (n + 1), 2):
238          true_row = temp_list[i]
239          true_probability = 1
240          false_probability = 1
241          for k in range(0, n, 1):
242              if true_row[k] == 'True':
243                  true_probability *= prob_list[k]
244                  false_probability *= 1 - prob_list[k]  # probability that mutation is false is 1 minus
245                  ↪   mutation is true
246
247          else:
248              true_probability *= 1 - prob_list[k]
249              false_probability *= prob_list[k]
250
251          final_true_probability = true_probability / (true_probability + false_probability)
252          final_false_probability = false_probability / (true_probability + false_probability)
253          temp_list[i].append(final_true_probability)
254          temp_list[i + 1].append(final_false_probability)
255
256  if __name__ == "__main__":
257      parser = argparse.ArgumentParser(description="train neural net")
258      parser.add_argument('-i', '--input', help="give directories with files")
259      paths = parser.parse_args()
260      main(paths)

```